Virus Research 266 (2019) 1–14

Contents lists available at ScienceDirect

Virus Research

journal homepage: www.elsevier.com/locate/virusres

Isolation and characterization of exosomes released from mosquito cells infected with dengue virus

José Manuel Reyes-Ruiz[a], Juan Fidel Osuna-Ramos[a], Luis Adrián De Jesús-González[a], Arianna Mahely Hurtado-Monzón[a], Carlos Noe Farfan-Morales[a], Margot Cervantes-Salazar[a], Jeni Bolaños[a], Oscar E. Cigarroa-Mayorga[e], Eduardo San Martín-Martínez[f], Fernando Medina[a], Rogelio Jaime Fragoso-Soriano[d], Bibiana Chávez-Munguía[a], Juan Santiago Salas-Benito[b,c], Rosa M. del Angel[a,*]

[a] Department of Infectomics and Molecular Pathogenesis, Center for Research and Advanced Studies (CINVESTAV-IPN), Mexico City, Mexico
[b] Maestría en Ciencias en Biomedicina Molecular, Escuela Nacional de Medicina y Homeopatía, Instituto Politécnico Nacional, Mexico City, Mexico
[c] Doctorado en Ciencias en Biotecnología, Escuela Nacional de Medicina y Homeopatía, Instituto Politécnico Nacional, Mexico City, Mexico
[d] Department of Physics, Center for Research and Advanced Studies (CINVESTAV-IPN), Mexico City, Mexico
[e] Departamento de Tecnologías Avanzadas, Unidad Profesional Interdisciplinaria en Ingeniería y Tecnologías Avanzadas del Instituto Politécnico Nacional, Mexico City, Mexico
[f] Centro de Investigación en Ciencias Aplicada y Tecnología Avanzada del Instituto Politécnico Nacional (CICATA-IPN), Mexico City, Mexico

ARTICLE INFO

Keywords:
Dengue virus
Exosomes
Intraluminal vesicles (ILVs)
Multivesicular bodies (MVBs)
C6/36 cells

ABSTRACT

Exosomes are endocytic origin small-membrane vesicles secreted to the extracellular space by most cell types. Exosomes released from virus infected-cells can mediate the cell-to-cell communication to promote or modulate viral transmission. Dengue virus (DENV) is an arbovirus transmitted by *Aedes* mosquitoes bite to humans. Interestingly, the role of exosomes during the DENV infection in mammalian cells has already been described. However, little is known about exosomes derived from infected mosquito cells. Thus, the exosomes released from DENV-infected C6/36 cells were isolated, purified and analyzed using an antibody against the tetraspanin CD9 from human that showed cross-reactivity with the homologs to human CD9 found in *Aedes albopictus* (AalCD9). The exosomes from DENV infected cells were larger than the exosomes secreted from uninfected cells, contained virus-like particles, and they were able to infect naïve C6/36 cells, suggesting that exosomes are playing a role in virus dissemination.

1. Introduction

Extracellular vesicles (EVs) are released by different types of cells and are classified according to size and the cell compartment from which they are originated (Delabranche et al., 2012). Thus, EVs are divided into apoptotic bodies (vesicles of 50–5000 nm formed during the apoptotic disintegration) (Cocucci et al., 2009; Gheinani et al., 2018; Kalra et al., 2012), microvesicles or ectosomes (vesicles of 50–1000 nm which bud directly from the plasma membrane) (Gheinani et al., 2018; Kalra et al., 2012), and exosomes (nanovesicles of 30–150 nm, originated from multivesicular bodies (MVBs)) (Gheinani et al., 2018; Kalluri, 2016; Li et al., 2014, 2017; Regev-Rudzki et al., 2013). The exosomes secretion occurs in many cells including dendritic (Théry et al., 1999), epithelial (van Niel et al., 2001), reticulocytes (Pan and Johnstone, 1983) and tumor cells (Azmi et al., 2013; Mears et al., 2004; Steinbichler et al., 2017) among others. These nanovesicles participate in physiological mechanisms and also during diseases such as viral infections (Bukong et al., 2014; Klibi et al., 2009; Meckes et al., 2010; Ramakrishnaiah et al., 2013).

Studies of exosomes produced from infected cells have shown highly specific exosome populations with distinct molecular repertoires which determine their roles in intracellular communication (Meckes, 2015). Exosomes released from cells infected with herpes simplex virus (HSV) contain functional viral tegument proteins and can enhance the infectivity of viral DNA (Dargan and Subak-Sharpe, 1997). The exosomes that come from hepatitis C virus (HCV)-infected cells contain viral RNA which facilitate infection of new cells (Ramakrishnaiah et al., 2013), while the dendritic cell infected-derived exosomes can mediate HIV-1 transmission (Wiley and Gummuluru, 2006). Additionally, exosomes produced from Epstein-Barr virus (EBV)-infected cells contain

* Corresponding author.
E-mail address: rmangel@cinvestav.mx (R.M. del Angel).

https://doi.org/10.1016/j.virusres.2019.03.015
Received 28 September 2018; Received in revised form 13 March 2019; Accepted 20 March 2019
Available online 28 March 2019

immunoregulator proteins such as IL-1b, IL-18, and IL-33 (Ansari et al., 2013), viral mRNAs (*v*mRNAs) (Canitano et al., 2013), EBV-encoded small RNAs (EBERs) (Ahmed et al., 2014), and the LMP2a protein (Ikeda and Longnecker, 2007; Meckes et al., 2013). Moreover, there is evidence that the exosomes are used by nonenveloped viruses as a novel pathway for cell-to-cell spread and immune system avoidance (Feng et al., 2013). Nonetheless, little is known about the role of exosomes in mosquito-borne viruses.

Dengue is an important arboviral infection caused by dengue virus (DENV) that contains four serotypes (DENV 1–4), belongs to the *Flavivirus* genus of the family *Flaviviridae* (Guzman and Harris, 2015; Simmons et al., 2012), and it is transmitted by *Aedes* mosquitoes (Kraemer et al., 2015). In this regard, the presence of mammalian cells-derived exosomes during DENV infection and their role in the intercellular transmission of mediators for anti-viral response have been previously reported (Martins et al., 2018; Zhu et al., 2015). Recently, the isolation and characterization of EVs from DENV-infected mosquito cells have also been reported (Vora et al., 2018). Vora et al. reported that DENV 2/DENV 3-infected cells secrete EVs with the size range from 30 to 250 nm, containing infectious viral RNA and proteins. The full-length genome of DENV 2 detected in EVs was able to infect mosquito and mammalian cells (Vora et al., 2018).

Given the importance of EVs in viral infection and since in the EVs fraction different types of vesicles are present, in this study we used various strategies such as negative staining electron microscopy, atomic force microscopy, and dynamic light scattering to isolate and characterize exosomes from DENV-infected C6/36 cells. Our results indicate that the exosomes from DENV infected cells were larger than the exosomes secreted from uninfected cells, contained virus-like particles and they were able to infect naïve C6/36 cells, suggesting that exosomes are playing a role in virus dissemination.

2. Materials and methods

2.1. Depletion of extracellular vesicles from fetal bovine serum

The fetal bovine serum (FBS) (Gibco) was ultracentrifuged at 100,000 × *g* for 80 min at 4 °C (Type 55.2 Ti rotor in a Beckman Optima™ L-60 Ultracentrifuge), and it was filtered through a 0.22 μm filter (Millipore) to remove the EVs.

2.2. Cell culture and viral strain

The C6/36 HT cells (Igarashi, 1978; Kuno and Oliver, 1989) were cultured in Minimal Essential Medium (Invitrogen) supplemented with 10% EVs-depleted FBS (Gibco), vitamins (Invitrogen), 0.034% sodium bicarbonate (J.T. Baker), 100 μg/mL streptomycin and 100 U/mL penicillin (Sigma).

DENV serotype 2 (New Guinea C strain), kindly donated by the Instituto de Diagnóstico y Referencia Epidemiológicos (InDRE, Mexico), was propagated in suckling Balb/c mice as described previously (Gould and Clegg, 1991). The viral titer was determined by plaque assay in BHK-21 cells (Juárez-Martínez et al., 2012). Brain extracts from uninfected suckling BALB/c mice were used as a control (mock-infected).

2.3. In silico and phylogenetic analysis of tetraspanins

The amino acids sequences of the tetraspanins CD9 (access number: hsa:928) and CD81 (access number: hsa:975) from the human were collected of the KEGG database (http://www.genome.jp/kegg/) and were used as query sequences in subsequent BLAST searches to identify CD9 and CD81 tetraspanin-like proteins in the database of *Aedes albopictus*, using VectorBase (https://www.vectorbase.org/), a Bioinformatics Resource for Invertebrate Vectors of Human Pathogens. The homologs to tetraspanins CD9 and CD81 from the human found in *A. albopictus*, AalCD9 (XP_019534275.1) and AalCD81 (XP_019527656.1) respectively, were aligned with the human CD9 and CD81 using the ClustalW software. Finally, the data were submitted to phylogenetic analysis by UPGMA using MEGA 5.05 software (Tamura et al., 2011). Additionally, bootstrapping was performed for 1000 replicates. The identity and e-value between AalCD9 and AalCD81 hypothetical proteins, compared with the CD9 and the CD81 orthologs, were determined using the Expert Protein Analysis System (ExPASy) of the Proteomic Analysis Server from the NCBI Blast service program (http://www.expasy.org/). Structural domains were identified using the SMART normal server (http://smart.emblheidelberg.de/), and the multiple alignments of the proteins were performed using T-COFFEE server (http://tcoffee.crg.cat/apps/tcoffee/do:expresso).

2.4. Proteins 3D modeling

The 3D structure prediction of AalCD9 and AalCD81 proteins was performed using the I-TASSER server (https://zhanglab.ccmb.med.umich.edu/I-TASSER/) and RaptorX (http://raptorx.uchicago.edu/StructurePrediction/predict/). Also, the orientation of AalCD9 and AalCD81 in the membrane was obtained *via* the OPM database (http://opm.phar.umich.edu/). The 3D AalCD9 and AalCD81 models were compared with the crystal structure of human CD81 (5TCX) retrieved from the Protein Data Bank (PDB). The 3D structures of proteins were visualized using the UCSF Chimera v1.10.1 software.

2.5. DENV infection

The C6/36 cells were mock-infected or DENV-infected at a MOI of 1 for 2 h at 35 °C. Then, the cells were washed with acid glycine (pH 3) to inactivate the non-internalized virus, and the infection was allowed to proceed for 24 h.

2.6. Cell viability assay

C6/36 cells seeded into 96-well plates (5×10^4 cells per well) were mock-infected or DENV-infected. The cell viability was analyzed using the CytoTox 96 non-radioactive cytotoxicity assay (Promega, Madison, WI) after 24 h, according to the manufacturer's instructions. The absorbance was measured at 490 nm with a plate reader (Multiskan FC, Thermo Scientific).

2.7. Confocal microscopy

The C6/36 cells were grown on coverslips placed in 24-well plates. After 24 h, cells were fixed with 1% formaldehyde, permeabilized for 20 min (0.1% saponin, 1% EVs-depleted FBS, and 1× PBS), and were incubated overnight at 4 °C with anti-CD9 (sc-59140, Santa Cruz), anti-CD81 (ab109201, Abcam), anti-prM/E DENV complex (ATCC® HB-114), or anti-Alix (kindly donated by Dr. Esther Orozco, Cinvestav, Mexico) antibodies. As secondary antibodies, donkey anti-mouse Alexa 488 or goat anti-rabbit Alexa 555 (Life Technologies) were used, and nuclei were counterstained with Hoechst (Santa Cruz). Finally, the slides were observed in a Zeiss LSM700 laser confocal microscopy, and the images were analyzed using the ZEN software, v. 2010.

2.8. Western blotting

The purified exosomes pellets were treated with RIPA buffer and protease inhibitors (Sigma–Aldrich). Fifty micrograms of protein extract were separated by a 12% SDS-PAGE in the presence of 2-mercaptoethanol and transferred to nitrocellulose membranes. The membranes (Whatman, Sigma–Aldrich) were incubated with anti-CD9 (1:400; Santa Cruz), anti-CD81 (1:500, Abcam), or anti-GAPDH (1:10,000, Cell Signaling); and secondary antibodies HRP-labeled goat anti-mouse or anti-rabbit IgG (1:10,000; System Biosciences). Finally, the proteins were detected using the Super Signal West Femto

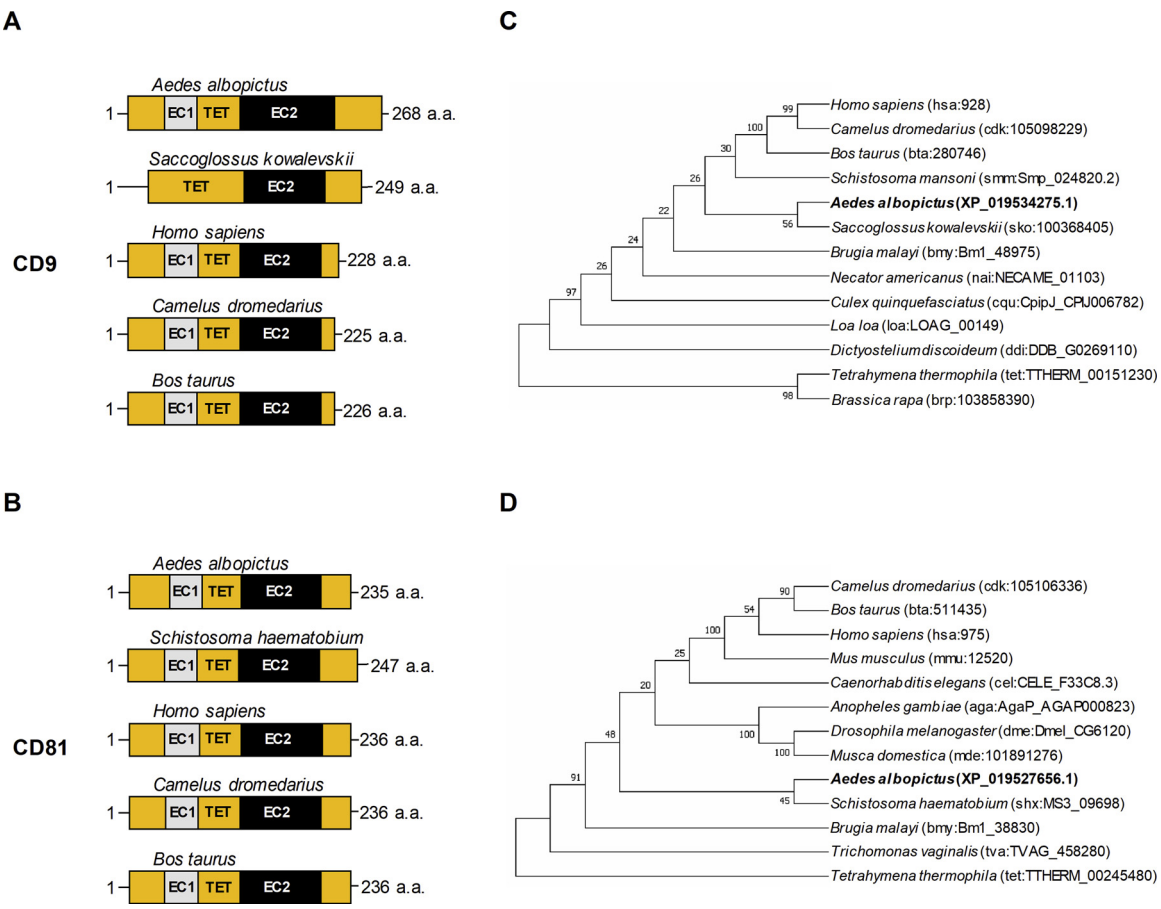

Fig. 1. Structural domains and phylogenetic trees of AalCD9 and AalCD81. Schemes show the main structural characteristics of tetraspanins CD9 (A) and CD81 (B) from distinct organisms. EC1: short extracellular loop, EC2: large extracellular loop, TET: tetraspanins domain. The numbers at the right correspond to the amino acids forming the proteins. (C and D) Phylogenetic tree indicating the composition of the proteins CD9 (C) and CD81 (D) of *Aedes albopictus* among different species. Numbers on horizontal lines in the trees indicate the confidence percentages of the tree topology from bootstrap of 1000 replicates.

Chemiluminescent Substrate (Thermo Scientific).

2.9. Transmission electron microscopy

The C6/36 cells grown in T-75 flasks (Corning) were mock-infected or infected with DENV 2 at a MOI of 1. We used DENV-infected C6/36 cells at a MOI 1 for 24 h because, at this time, a higher amount of MVBs were detected compared to 48 hpi (data not shown). Then, the samples were fixed with 2.5% glutaraldehyde in 0.1 M sodium cacodylate buffer pH 7.2 for 1 h at room temperature (RT), and post-fixed with 1% osmium tetroxide for 1 h at RT. The samples were dehydrated through an ethanol gradient and propylene oxide, and then they were embedded in Polybed epoxy resins and polymerized at 60 °C for 24 h. Finally, 70-nm thin sections were stained with uranyl acetate and lead citrate and were analyzed using a Jeol JEM-1011 transmission electron microscope (Jeol Ltd., Tokyo, Japan).

2.10. Isolation of exosomes from the cell culture supernatant

The supernatants from mock-infected and DENV-infected C6/36 cells were collected after 24 h and centrifuged using a Sorvall® H-400 centrifuge at 300 × *g* for 10 min to remove cells. The supernatants were collected and centrifuged at 2000 × *g* for 10 min and 10,000 × *g* for 1 h at 4 °C (Beckman Coulter Avanti® J-26 XP centrifuge/JA-25.50 rotor) and filtered through 0.22 µm filter (Merck Millipore). Then, the clarified supernatants were recovered and ultracentrifuged at 100,000 × *g* for 80 min at 4 °C with a Type 55.2 Ti rotor in a Beckman Optima™ L-60 Ultracentrifuge. The supernatants were removed as thoroughly as possible, and the pellets were resuspended in 1 mL of PBS, pooled, and once again ultracentrifuged at 100,000 × *g* for 80 min at 4 °C. Finally, the PBS was discarded entirely, and the exosomes were resuspended in PBS. Immediately, the exosomes were treated with Total Exosome Isolation Reagent (Invitrogen Life Technologies) according to the manufacturer's instructions to concentrate intact exosomes. The mixture of the exosomes and reagent was incubated at 4 °C overnight and centrifugated at 10,000 × *g* for 1 h at 4 °C. Afterward, the Dynabeads (Exosome Immunoprecipitation Reagent (Protein A), Invitrogen Life Technologies) were resuspended with the anti-CD9 antibody (Ab) in 200 µL PBS with Tween-20 during 10 min at RT. The samples were placed on the magnet for 1 min, and the supernatant (DENV fraction) was collected in a clean tube. The beads-Ab complex was resuspended in 200 µL PBS with Tween-20, mixed with the exosomes (Exo) contained in the pellet and were incubated for 1 h at RT. The Dynabeads-Ab-Exo complex was washed three times using the magnet, resuspended in 200 µL elution buffer (50 mM glycine, pH 2.8) and incubated for 2 min at RT to dissociate the complex. Finally, the samples were placed on the magnet for 1 min, and the supernatants with the exosomes eluted were collected in a clean tube and analyzed by negative staining electron microscopy to confirm their purity.

2.11. Negative staining electron microscopy analysis

The purified exosomes and preparation of DENV particles (DENV fraction) were placed on the surface of the formvar-coated copper grids and stained with 2.5% uranyl acetate. The grids were allowed to dry, coated with carbon and then examined through a JEM-1011

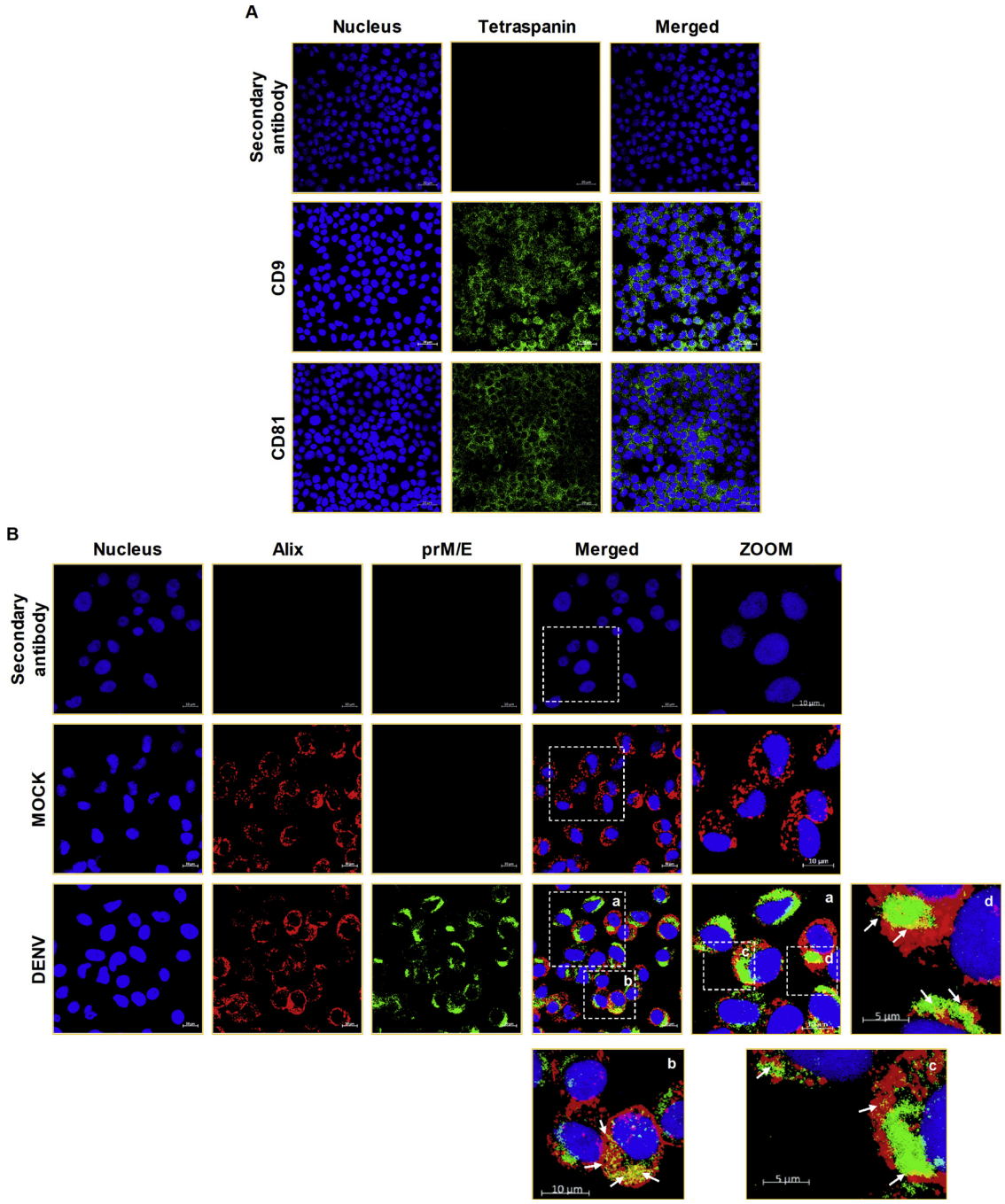

Fig. 2. Identification of tetraspanins and Alix in C6/36 *Aedes albopictus* cells. (A) The recognition of mosquito tetraspanins, homologs to the human tetraspanins CD9 and CD81, was evaluated by confocal microscopy using the human anti-CD9 and anti-CD81 antibodies (green). (B) The distribution of Alix (red) and viral protein prM/E (green) in mock or DENV-infected C6/36 cells was analyzed by confocal microscopy. The a, b, c and d images are ZOOM of cells. Nuclei were stained with Hoechst (blue). The secondary antibody was used as isotype control to assess the specificity of the reaction appropriately. (For interpretation of the references to color in this figure legend, the reader is referred to the web version of this article.)

transmission electron microscope.

2.12. Viral infection assay

C6/36 cells were mock infected, infected with DENV 2 (DENV fraction obtained during the exosomes purification), or treated with the exosomes released from uninfected or infected C6/36 cells for 24 h. Afterward, the cells were fixed at RT for 20 min with 1% formaldehyde, were permeabilized for 20 min with permeabilizing solution and were incubated with anti-prM/E DENV complex for 2 h at RT. As secondary antibody, a goat anti-mouse Alexa Flour 488 (Life Technologies) was used. Flow cytometry was performed in a BD LSR Fortessa™, and the data were analyzed using the FlowJo v. 10 software.

2.13. Atomic force microscopy

Exosomes from mock-infected and DENV-infected C6/36 cells were diluted with deionized water. Twenty microliters of each sample were deposited on a cleaned glass slide, and the drop was air dried for 15 minutes. Samples were analyzed by an atomic force microscope (Autoprobe CP Research, Thermo-microscopes, USA) in contact mode using a 1 µm scanner and 10 nm radius silicon nitride tip, mounted on a

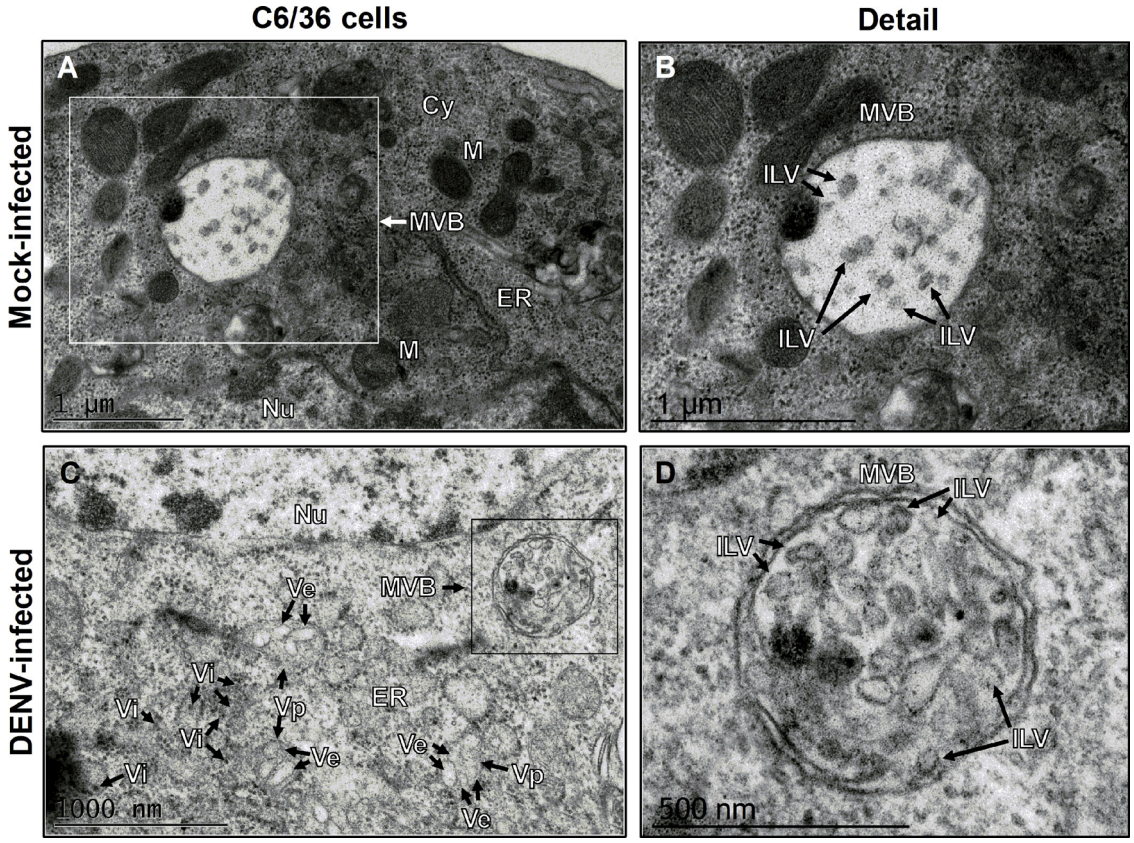

Fig. 3. DENV replication complexes are close to MVBs in C6/36 cells infected. The TEM analysis of mock (A and B) and DENV-infected (C and D) C6/36 cells at 24 h post-infection. MVB, multivesicular body; ILV, intraluminal vesicle; Nu, nucleus; M, mitochondria; Cy, cytoplasm; ER, endoplasmic reticulum; Ve, double-membrane vesicles; Vp, membrane packets; Vi, virus-like particles.

0.6 µm ultralever model SNL-10 (Veeco Probes, CA). A scan rate of 0.8–1 Hz, a force of 6 nN, and a gain of 0.5 arbitrary units were used. Images and analysis of height profiles and structures diameters were generated with ProScan software (version 1.9, Park Scientific Instruments, 2005).

2.14. Dynamic light scattering

The average size of exosomes was determined by dynamic light scattering principle using a MALVERN Zetasizer Nano ZS (Malvern, Herrenberg, Germany). The measurements were performed at RT; both samples: exosomes derived from mock and DENV-infected C6/36 cells were resuspended in milli-Q water at a rate of 2:200. The area under the curve was calculated in triplicate for each sample by the known numerical approximation method according to the following equation and assuming that the distributions are continuous functions in $[a, b]$ interval.

$$A = \frac{b-a}{2n}\left[f(a) + 2\sum_{k=1}^{n-1} f(x_k) + f(b)\right]$$

The samples were put in the Malvern measurement cell and run into the scattering procedure. To determine the stability of the exosomes, the potential zeta was measured for each sample in the MALVERN Zetasizer using the same above described condition.

2.15. Statistical analysis

The size of the exosomes produced from Mock- and DENV-infected C6/36 cells was determined from a profile of the negative stain electron microscopy and atomic force microscopy images, and the dynamic light scattering analysis. The graphs were represented as a scatter dot blot with mean and the standard error of the mean (SEM). *P* values were determined by unpaired *t*-test with Welch's correction using the GraphPad Prism software version 6.0. Considering as significant value when $p < 0.05$, to indicate a statistical difference.

3. Results

3.1. Aedes albopictus possess tetraspanin-like proteins

Since tetraspanins such as CD9 and CD81 are constitutive components and proteins enriched in the exosomes (Andreu and Yáñez-Mó, 2014), the presence of proteins similar to the tetraspanins CD9 and CD81 from the human in *A. albopictus* were analyzed *in silico*. The search was performed in the VectorBase (https://www.vectorbase.org/) and revealed the presence of a 268 amino acids sequence with 16.59–34.33% identity to CD9 proteins of different species (Fig. 1A and Supplemental material Table S1). Also, the *in silico* analysis demonstrated the presence of a sequence of 235 amino acids with 15.09–31.11% of identity to other CD81 proteins (Fig. 1B and Supplemental material Table S2). The putative proteins CD9 (AalCD9) and CD81 (AalCD81) from *A. albopictus* exhibited the four hydrophobic transmembrane regions (TM1–TM4), the short extracellular loop (EC1), and a large extracellular loop (EC2) domains which are found in the tetraspanins CD9 and CD81 (Hemler, 2005; Kitadokoro et al., 2001; Stipp et al., 2003).

The full-length sequences of the proteins AalCD9 and AalCD81 were compared to the full-length sequences of the tetraspanins CD9 and CD81 from other organisms to construct phylogenetic trees using the MEGA 5.05 software. The AalCD9 sequence was grouped in a single clade with the hemichordate *Saccoglossus kowalevskii*, in the branch of the mammals such as *Homo sapiens* and *Bos taurus*, and a parasitic

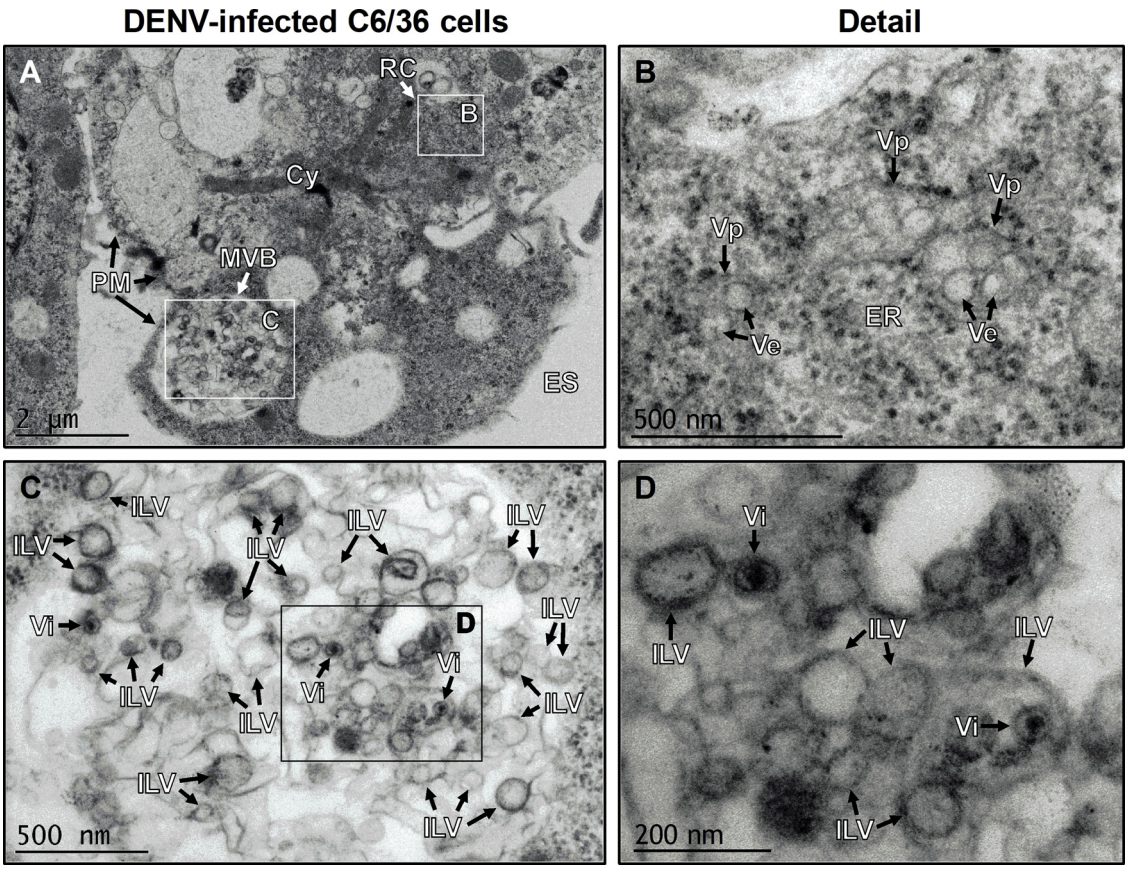

Fig. 4. MVB close to the plasma membrane of DENV-infected cells. (A–D) The TEM analysis of DENV-infected C6/36 cells at 24 h post-infection. The replicative complexes (B), MVB (C), and virus-like particles inside the intraluminal vesicle (D) are shown. MVB, multivesicular body; ILV, intraluminal vesicle; Cy, cytoplasm; ER, endoplasmic reticulum; ES, extracellular space; PM, plasma membrane; RC, replication complexes; Ve, double-membrane vesicles; Vp, membrane packets; Vi, virus-like particles.

helminth *Schistosoma mansoni*; far from the hypothetical CD9 of protozoa such as *Dictyostelium discoideum* and *Tetrahymena thermophila* (Fig. 1C). On the other hand, the AalCD81 was found linked to the helminth *Schistosoma haematobium*, in the branch of mammals (*H. sapiens*, *Camelus dromedarius*, *B. taurus*, and *Mus musculus*) and insects (*Anopheles gambiae*, *Drosophila melanogaster*, and *Musca domestica*) (Fig. 1D).

To obtain further evidence of the structural relationship of the proteins AalCD9 and AalCD81 with their orthologs, 3D models were constructed using I-TASSER server (https://zhanglab.ccmb.med.umich.edu/I-TASSER/). The crystal structure of the human tetraspanin CD9 is not available; thus the crystal structure of the full-length human tetraspanin CD81 (Zimmerman et al., 2016) was used for the comparative analysis of the protein structures. The predicted 3D structure analysis of the proteins AalCD9 and AalCD81 showed the same crystal (HsaCD81; 5TCX) and presented 89.6% and 87% of structural identity to the crystal structure of the human tetraspanin CD81 (Zimmerman et al., 2016), respectively (Supplemental material Fig. S1A). Also, the 3D models of the AalCD9 and AalCD81 were analyzed by the Orientation of Proteins in Membranes (OPM) database (http://opm.phar.umich.edu/) and the EC2 domain topologically was located between TM3 and TM4, and showed five α-helices such as the human tetraspanin CD81 (Zimmerman et al., 2016) (Supplemental material Fig. S1B). On the other hand, the alignment by ClustalW (UCSF Chimera v1.10.1 software) of the amino acids sequences of AalCD9, AalCD81, HsaCD9, and HsaCD81 revealed the presence of the four invariant Cys residues, two of which define the conserved Cys-Cys-Gly motif and other two localized through the sequence in the EC2 (AalCD9: 107–231 a.a.; AalCD81: 110–205 a.a.; HsaCD9: 112–192 a.a., and HsaCD81: 113–201 a.a.) (Supplemental material Fig. S2); which are characteristic of the human tetraspanins CD9 and CD81 (Hemler, 2005; Kitadokoro et al., 2001; Stipp et al., 2003).

In summary, the bioinformatics analysis showed that the proteins AalCD9 and AalCD81 have sequence and structural similarities to their orthologs in human (tetraspanins CD9 and CD81), suggesting that *A. albopictus* possess tetraspanin-like proteins.

3.2. Identification of multivesicular bodies-like structures in C6/36 cells

Since for cell cultures, the fetal bovine serum (FBS) was depleted of EVs; the first step was to determine the cell viability under these conditions. In the presence of the EVs-depleted FBS, the cell viability of mock and DENV-infected C6/36 cells was not altered (Supplemental material Fig. S3). Then, since the *in silico* analysis suggested the presence of tetraspanins-like proteins in *A. albopictus*, the presence of tetraspanins in the C6/36 *A. albopictus* cells was confirmed by confocal microscopy analysis using antibodies against the human tetraspanins CD9 and CD81. A cytoplasmic staining pattern of the tetraspanins CD9 and CD81 was observed in the C6/36 cells (Fig. 2A). This pattern has also been observed by immunofluorescence assays in mammalian cells (Chang and Finnemann, 2007; Imhof et al., 2008; Kaji et al., 2001; Meyer et al., 2015). Tetraspanins CD9 and CD81 are constitutive components of exosomes (Berditchevski and Odintsova, 2007; Escola et al., 1998; Mathivanan et al., 2010), which are formed as intraluminal vesicles (ILVs) into MVBs and these are released by the fusion between the MVBs and the plasma membrane (PM) (Simons and Raposo, 2009). Since Alix is a protein involved in the ILVs formation (Bissig and Gruenberg, 2014), mock and DENV-infected cells were labeled with

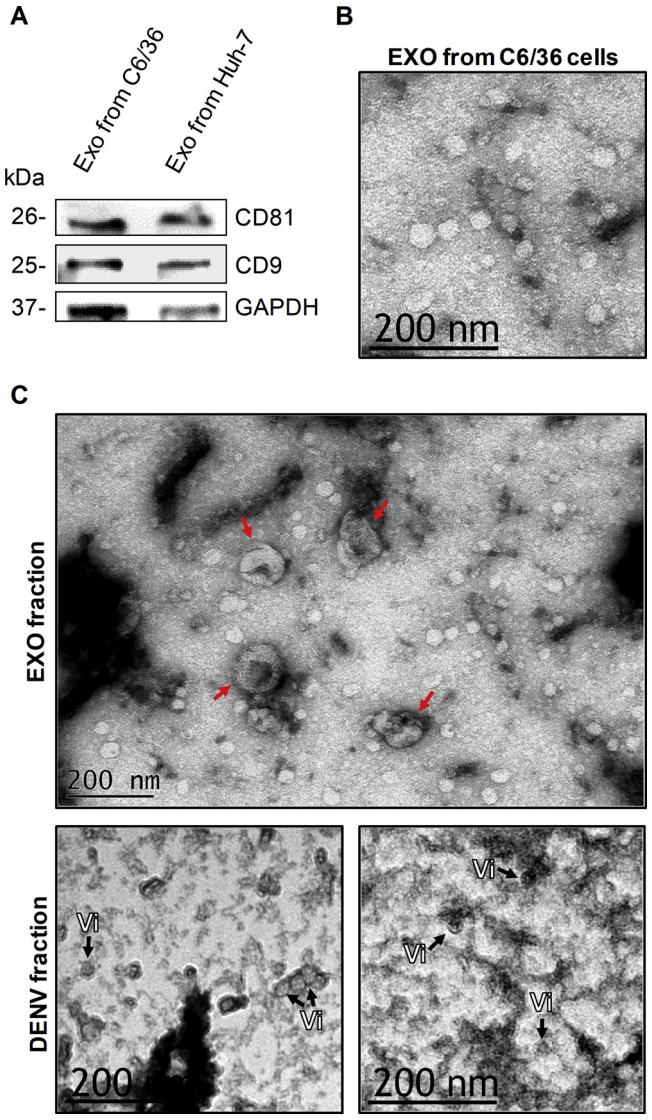

Fig. 5. Isolation of exosomes derived from DENV-infected C6/36 cells. (A) Exosomes released from C6/36 and Huh-7 cells were isolated by differential ultracentrifugation and analyzed by western blot using the human anti-GAPDH, anti-CD9, and anti-CD81 antibodies. (B) Exosomes were observed by negative staining electron microscopy. (C) Observation of the exosomes purified from DENV-infected C6/36 cells (exosomal fraction), and the DENV fraction. The exosomes are observed as spherical structures with "cup-like" shaped (indicated by red arrows). EXO, exosomes; Vi, virus-like particles.

anti-Alix and anti-prM/E antibodies and analyzed by confocal microscopy. The Alix protein was localized in the cytoplasm and in the perinuclear region of the cells in both conditions, suggesting the presence of ILVs in C6/36 cells. In contrast, the prM/E protein was only observed in the perinuclear region of DENV-infected C6/36 cells (Fig. 2B). This viral protein co-localized with Alix in some infected cells, suggesting that prM/E and Alix can be present in the same compartment (Fig. 2B (b, c and d)). To confirm the presence of MVBs-like structures in C6/36 cells, a Transmission Electron Microscopy (TEM) analysis was performed. In mock-infected C6/36 cells, we observed MVBs-like structures of ~1 μm diameter that enclosed small vesicles with diameters from 45 to 60 nm (Fig. 3A and B), as has been previously described for mammalian cells (Edgar, 2016; Scotti et al., 2013; Von Bartheld and Altick, 2011). These MVB-like structures were visualized in ultrathin sections as spherical organelles with a single or double outer (limiting) membrane and with a freely variable number of small spherical or ellipsoidal vesicles in a electron lucent matrix (An et al., 2006a, 2006b; Chivet et al., 2012; Edgar, 2016; Tamboli et al., 2010; Von Bartheld and Altick, 2011), in contrast to what is observed in autophagosomes, which are vacuoles that surrounded part of the cytoplasm or organelles (Pandey et al., 2007). Interestingly, the MVBs in DENV-infected C6/36 cells (with diameters from 0.6 to 2.2 μm) contained many small vesicles like the ILVs of diameters in a broader range from 60 to 150 nm (Fig. 3C and D). A notable finding was that the infected cells contained MVBs and ILVs larger than those observed in uninfected cells. Moreover, MVBs were found close to the DENV-induced intracellular membrane structures in the endoplasmic reticulum (ER) such as the spherical vesicles of 80–90 nm called double-membrane vesicles (Ve) enclosed within membrane packets (Vp). These replicative complexes are sites of viral replication, assembly, and budding as have been previously reported in DENV-infected cells (Junjhon et al., 2014; Reyes-Ruiz et al., 2019, 2018; Welsch et al., 2009) (Fig. 3C). Also, spherical electron-dense structures of ~50 nm diameter with a membranous layer which looks like viral particles (Vi, virus-like particles) (Reyes-Ruiz et al., 2019, 2018; Welsch et al., 2009) were found (Fig. 3C). Finally, the presence of MVBs close to the PM in DENV-infected C6/36 cells were identified, suggesting that ILVs could be released into the extracellular space as exosomes (Fig. 4A), as has been reported by transmission electron microscopy in previous studies (Colombo et al., 2014; Hyenne et al., 2015; Tamboli et al., 2010; Urbanelli et al., 2013). Additionally, replicative complexes were observed in the infected cells (Fig. 4B) and the Vi were localized in the MVB and inside of ILVs (Fig. 4C and D).

3.3. Isolation and morphological characterization of the exosomes derived from DENV-infected cells

The TEM analysis suggested that the exosomes could be released to the extracellular space. To confirm this possibility, the exosomes derived from DENV-infected and mock-infected C6/36 cells were isolated from the supernatant by a series of ultracentrifugation steps based on a previously described method (Théry, 2011). To verify the efficiency of the method used, the exosomes released from C6/36 cells were examined by western blot and negative stain electron microscopy. The antibodies against the tetraspanins CD9 and CD81 from human were able to detect by western blot the proteins AalCD9 and AalCD81 in the exosomes derived from C6/36 cells, supporting the idea that they contain tetraspanins like the human exosomes (Fig. 5A). Also, GAPDH an exosome marker protein (Jella et al., 2016; Yang et al., 2017) was also detected in the exosomes released from C6/36 cells (Fig. 5A). As a positive control, exosomes produced from Huh-7 cells were obtained and analyzed by western blot (Fig. 5A). On the other hand, the electron microscopy analysis revealed spherical structures of ~40 nm (Fig. 5B) that were morphologically similar to exosomes released from eukaryotic cells (Muller et al., 2014; Pisitkun et al., 2004).

Moreover, to obtain exosomes with higher purity and to eliminate the viral contamination, in the case of the exosomes from infected cells, we used ultracentrifugation combined with anti-CD9 immunomagnetic bead affinity purification. The purified exosomes were further analyzed by electron microscopy using negative staining (Fig. 5C). Since the morphological appearance of the exosomes is different from the virus-like particles, it was relatively easy to identify them (Fig. 5C). Ten different fields were analyzed in three different experiments by duplicate, and no viral particles were detected in the exosomal fraction (Fig. 5C), supporting the purity of the exosomal preparation. The exosomes produced from DENV-infected C6/36 cells had an average size of 81.18 nm and spherical structure with "cup-like" shaped (Fig. 5C) while the virus-like particles were observed as structures spherical-shaped and ~55 nm diameter (Fig. 5C).

Also, we found that the mean (± SEM) of exosomes size released from DENV-infected C6/36 cells was 81.18 nm (± 4.70) in contrast with the exosomes produced by mock-infected cells that had 46.77 nm (± 2.98) ($p =$ < 0.0001) (Fig. 6A and B). Some of the exosomes of

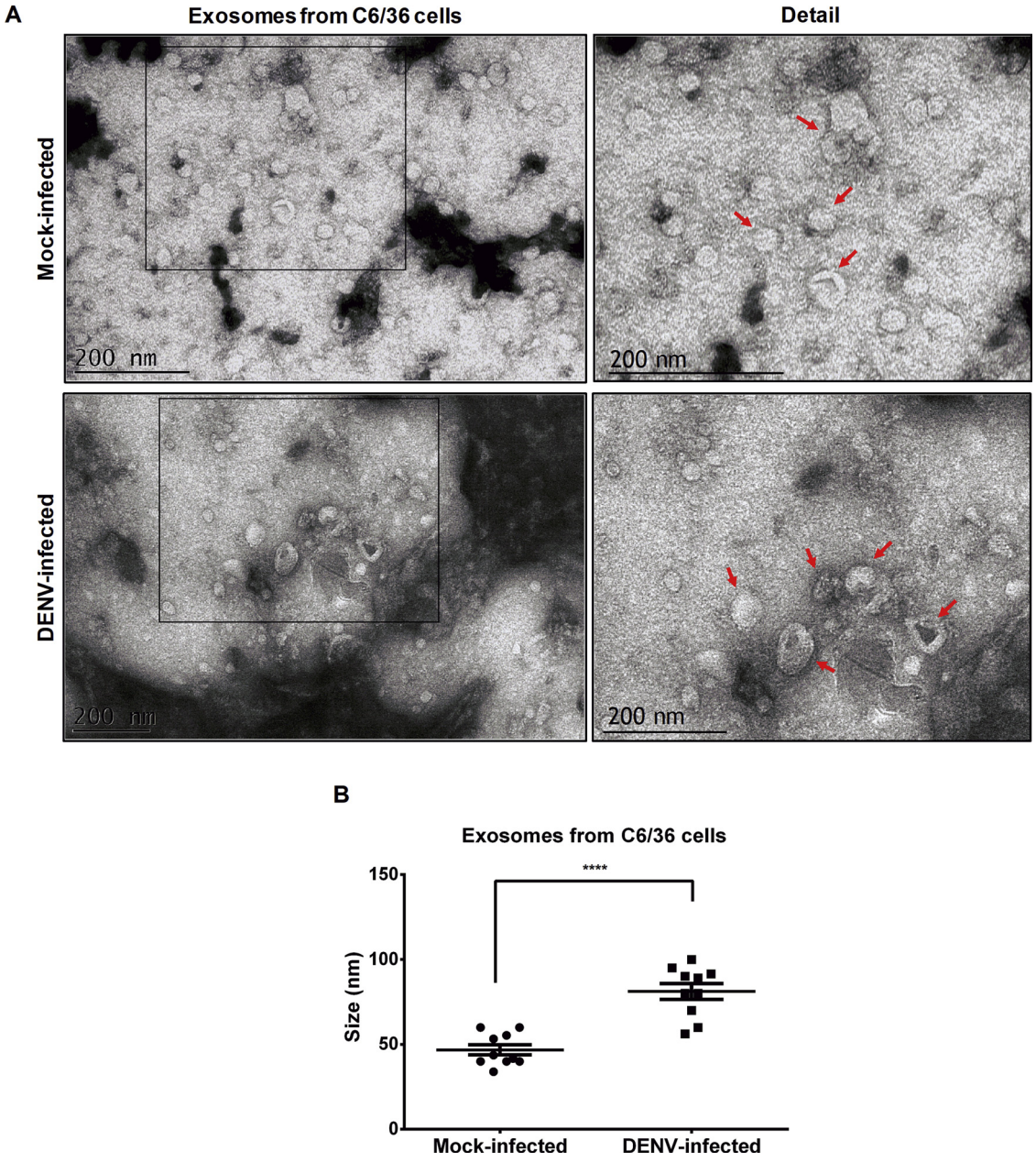

Fig. 6. The exosomes released from DENV-infected C6/36 cells are larger than the ones released by uninfected cells. (A) Exosomes derived from mock and DENV-infected C6/36 cells were analyzed and counted by negative staining electron microscopy. (B) The graph compares the size of the exosomes where each point in the graph represents fifty exosomes. The exosomes are observed as spherical structures with "cup-like" shape (indicated by red arrows). (For interpretation of the references to color in this figure legend, the reader is referred to the web version of this article.)

~100 nm derived from DENV-infected C6/36 cells enclosed structures spherical-shaped with ~55 nm diameter similar to DENV particle (Fig. 7A) (Kuhn et al., 2002). This result supports the observation performed in Fig. 4D where virus-like particle could be contained in the ILV. To determine the role of the exosomes produced from DENV-infected C6/36 cells, naïve C6/36 cells were incubated with these exosomes, and the percentage of infected cells was analyzed by flow cytometry. Interestingly, the exosomes released during DENV infection can infect naïve C6/36 cells as the purified DENV (without exosomes) (Fig. 7B) suggesting that the exosomes released from DENV-infected C6/36 cells have an infective potential. This result supports the idea that exosomes are playing a role in viral dissemination.

On the other hand, to corroborate the difference in the size of the exosomes released from uninfected and DENV-infected cells and evaluate their native structure, an atomic force microscopy (AFM) analysis (Fig. 8A and B) was performed. In six fields we counted 300 exosomes, and the exosomes derived from mock and DENV-infected cells were observed as vesicles with round-shape in a 3D topographic image (Fig. 8C and D) according to previous AFM studies performed on exosomes (Palanisamy et al., 2010; Sharma et al., 2010). Moreover, consistent with electron microscopy analysis, the size of the exosomes was different between the populations released from mock (exosomes of 43–65 nm diameter (mean ± SEM, 55.91 ± 2.71)) and DENV-infected C6/36 cells (exosomes of 55–150 nm diameter (mean ± SEM, 95.07 ± 13.34)) ($p = 0.0258$) (Fig. 8E). To further support this observation a dynamic light scattering (DLS), a technique for the analysis of nanoparticles was performed using a Malvern Zetasizer Nano ZS. The analysis showed that the mean (± SEM) of the exosomes size released from DENV-infected cells was 97.19 (± 10.50) in contrast with the mean of the exosomes derived from mock-infected cells, which was

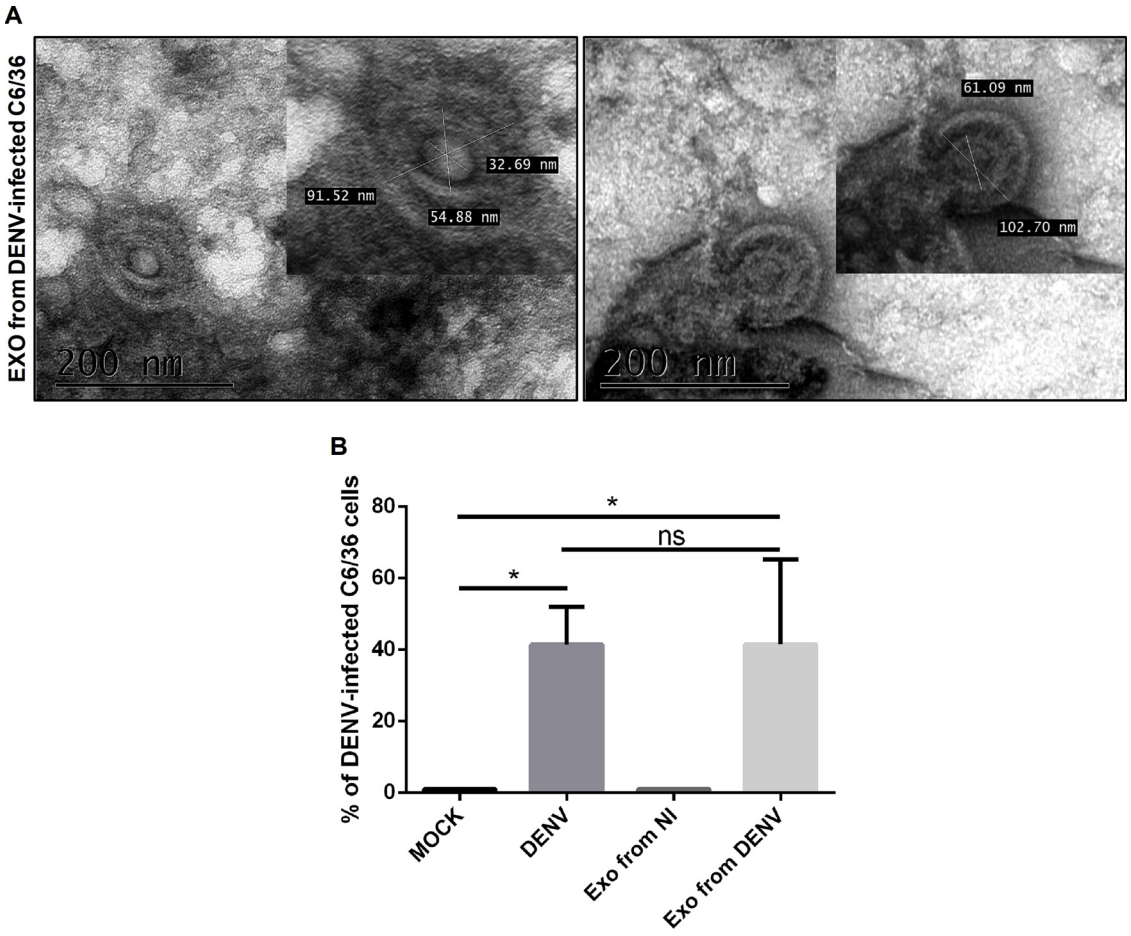

Fig. 7. Exosomes produced from DENV-infected C6/36 cells enclosed virus-like particles. (A) Exosomes (EXO) of ~100 nm derived from DENV-infected C6/36 cells enclosed structures spherical-shaped with ~55 nm diameter like the DENV particle. (B) Naïve C6/36 cells were treated with the exosomes released from uninfected (Exo from NI) and DENV-infected (Exo from DENV) C6/36 cells and the percentage of infection was analyzed by flow cytometry.

42.77 (± 2.29) (p = 0.0030) (Fig. 9A and B). Thus, the difference in sizes between the exosomes produced by mock and DENV-infected cells was significant.

Together, these results support the idea that the mosquito cells can produce and release exosomes, which contain tetraspanins as it has been described for the exosomes from mammalian cells. On the other hand, the exosomes released from DENV-infected C6/36 cells are larger than the ones released from mock-infected cells, contain virus-like particles, and they can infect naïve C6/36 cells.

4. Discussion

The exosomes secretion occurs in many cell types including dendritic (Théry et al., 1999), epithelial (van Niel et al., 2001), reticulocytes (Pan and Johnstone, 1983) and tumor cells (Azmi et al., 2013; Mears et al., 2004; Steinbichler et al., 2017) among others. These nanovesicles can transfer proteins, mRNA, and microRNAs to neighboring or distant cells contributing in the modulation of physiological processes or during infections (Bukong et al., 2014; Klibi et al., 2009; Meckes et al., 2010; Ramakrishnaiah et al., 2013). Consequently, it is possible that viruses exploit the exosomal pathway to spread infection and modify their target cells (Bobrie et al., 2011; Pegtel et al., 2011) or the cells use this mechanism to send signals to neighbor cells for the maintenance of cellular homeostasis (Baixauli et al., 2014; Braicu et al., 2015).

DENV is an arbovirus transmitted by *Aedes* mosquitoes bite to humans (Kraemer et al., 2015) and that requires different factors to replicate in the host cell (Reyes-Ruiz et al., 2019). It has recently been described that EVs derived from DENV-infected mammalian cells mediate the secretion of bioactive molecules, key to the host defense (Martins et al., 2018; Zhu et al., 2015). In contrast, the EVs isolated from DENV-infected mosquito cells contain infectious viral RNA and proteins being the full-length genome of DENV, infectious to mosquito and mammalian cells (Vora et al., 2018). These results suggest that while in mammalian cells the exosomes are playing an anti-viral role, the EVs have a pro-viral activity in mosquito cells. To further characterize the activity of a specific population of EVs, the exosomes, in mosquito cells, we isolated exosomes using the ultracentrifugation and later an immunoprecipitation assay using the CD9 specific marker of exosomes. As expected, we isolated a population of vesicles with a size range from 55 to 150 nm positive to the tetraspanins CD9. These vesicles have different size range than the ones isolated by Vora et al. (size range from 30 to 250 nm) which were isolated using OptiPrep and ultracentrifugation protocols (Vora et al., 2018).

The membranes of the exosomes contain sphingomyelin and cholesterol (Matsuo et al., 2004) an essential molecule during flavivirus infection (Osuna-Ramos et al., 2018), as well as the tetraspanins family proteins CD9 and CD81 which are used as markers of exosomes (Andreu and Yáñez-Mó, 2014). These tetraspanins play a role in many biological processes, *e.g.*, CD81 has an essential function in the immune system (Levy, 2014; van Spriel, 2011), whereas CD9 participates in fertilization process (Hemler, 2001; Jankovičová et al., 2015). In mammals, it has been reported 28 distinct family members of tetraspanins, but they are not exclusive of mammals since in *Drosophila* are known 37 members and 20 in *C. elegans* (Todres et al., 2000). The tetraspanins have certain features that differentiate them from other proteins such as four

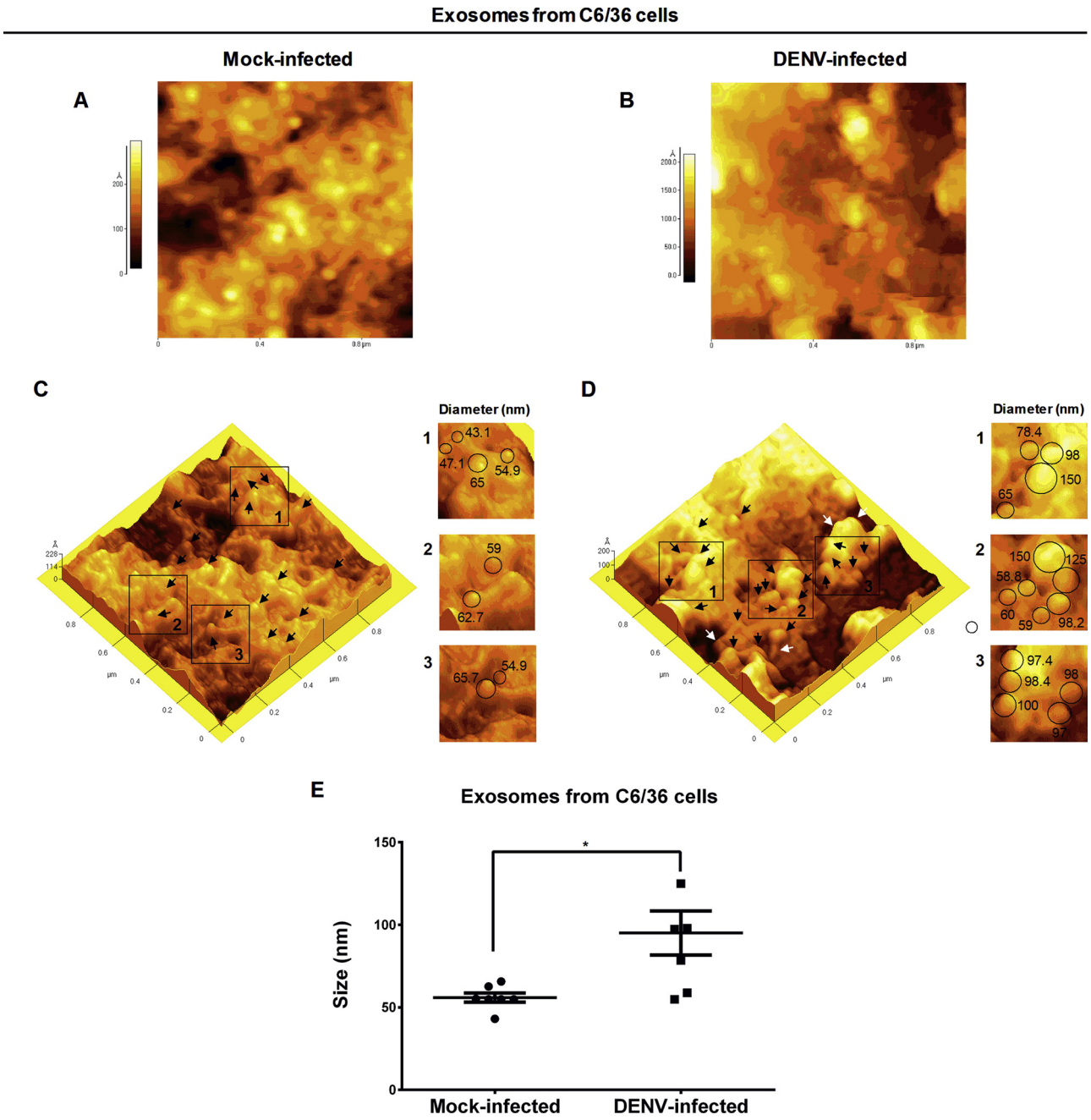

Fig. 8. The topography of the exosomes derived from mock and DENV-infected C6/36 cells. Exosomes produced by mock (A and C) and DENV-infected C6/36 cells (B and D) were observed under contact mode atomic force microscopy. The populations of exosomes were observed in 2D (A and B) and 3D images (C1, 2, and 3; and D1, 2, and 3) as structures of round-shaped (indicated by black and white arrows, and black circles). (E) The graph compares the diameter of the exosomes where each point in the graph represents fifty exosomes.

transmembrane domains, one short extracellular loop (EC1) and one large extracellular loop (EC2) which contain an essential conserved CCG motif where the epitopes recognized by monoclonal antibodies are located (Hemler, 2005). Moreover, the alignment between different tetraspanins from human and insect has shown conserved key residues such as CCG in the EC2; which makes possible to identify members of the tetraspanin family (Hemler, 2001). The search on VectorBase identified two proteins in *A. albopictus* C6/36 cell line as putative orthologs of the human tetraspanins CD9 and CD81 which were named AalCD9 and AalCD81, respectively. Using *in silico* analysis, we showed here that the tetraspanins identified in mosquito cells have similar characteristics to the human CD9 and CD81 tetraspanins. The mosquito tetraspanins homologs to the human tetraspanins CD9 and CD81 were recognized by human anti-CD9 and anti-CD81 antibodies respectively. This cross-reactivity shown by the human antibodies is due to a large epitope region in the EC2 of the tetraspanins in arthropod and vertebrate (Hemler, 2005). Moreover, the cross-reactivity of a human anti-tetraspanins CD63 antibody with tetraspanins contained in EVs secreted by mosquito cells has been shown previously (Vora et al., 2018). Thus, there is sufficient evidence to conclude that the mosquito cells contain proteins similar to tetraspanins.

On the other hand, the exosomes are nanovesicles (30–150 nm) of endocytic origin formed by the inward budding of MVBs, contrasting with other types of extracellular vesicles (microvesicles or ectosomes, and apoptotic bodies) secreted by the cells (Gheinani et al., 2018; Keerthikumar et al., 2016). TEM analysis in both uninfected or DENV-

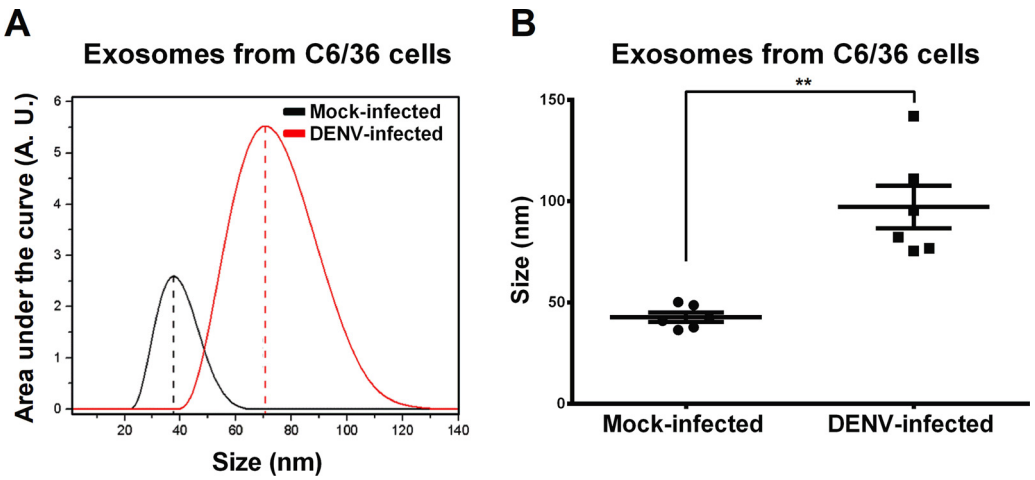

Fig. 9. Analysis of exosomes by dynamic light scattering. (A and B) The size distribution of exosomes released from mock and DENV-infected C6/36 cells was characterized using dynamic light scattering method.

infected C6/36 cells revealed structures with an MVB-like morphology that contained ILVs. These structures are consistent with the observation of MVBs in *A. albopictus* cells (Raghow et al., 1973). Also, we observed the presence of MVB-like structures close to the surface of the cells suggesting that they could release the ILVs into the extracellular space as exosomes, as has been described before (Hyenne et al., 2015; Tamboli et al., 2010; Théry et al., 1999; Zitvogel et al., 1998).

The exosomes are conventionally isolated from the cell culture supernatant or bodily fluids following sucrose-gradient and ultracentrifugation method (Théry et al., 2006). However, in the context of DENV-infected cells, the viral particles have a similar size to the exosomes, then it is difficult to separate the two populations. Therefore, the separation of exosomes from virions by positive selection using magnetic beads coupled to an antibody against a protein enriched in exosomes is by far the best method (Raab-Traub and Dittmer, 2017). In this study, the isolated exosomes from DENV-infected cells were purified by an anti-CD9 immunomagnetic bead, and the electron microscopy analysis confirmed that there were no free DENV particles in the purified exosomes.

Also, the purified exosomes of both infected and uninfected cells varied considerably in size. This result was consistent with previous reports that cells in different conditions secrete a heterogeneous population of exosomes with different sizes (Bobrie et al., 2012; Willms et al., 2016); thus corroborates the observations made here and the previously reported that within MVBs, ILVs are not all similar in size and morphology (Fevrier et al., 2004; Möbius et al., 2002; White et al., 2006). In this sense, exosomes secreted from DENV-infected C6/36 cells were larger than the ones released by mock-infected cells. The size variation could be due to the content of the exosomes produced from uninfected and infected cells due to the different stimulus and conditions of growth; as has been observed with the proteomic analysis of exosomes secreted at different stages of reticulocyte maturation (Carayon et al., 2011).

In this study, the exosomes isolated from DENV-infected C6/36 cells had a cup-shaped and round-shaped in the TEM and AFM analysis respectively similar to exosomes present in human body fluids (Palanisamy et al., 2010; Sharma et al., 2010). They also had diameters from 55 to 150 nm in accordance with the reported size range (Gheinani et al., 2018; Kalluri, 2016; Li et al., 2014, 2017; Regev-Rudzki et al., 2013) in contrast with the EVs of up to 350 nm reported by Vora et al. (2018).

An interesting finding here was the observation of virus-like particles enclosed in exosomes released from DENV-infected mosquito cells. Previous reports indicate that exosomes can carry and deliver viruses into recipient cells, as shown for the hepatitis C virus (Cosset and Dreux, 2014; Greenhill, 2013; Longatti et al., 2015; Ramakrishnaiah et al., 2013), tick-borne encephalitis virus (TBEV) (Zhou et al., 2018), human immunodeficiency virus type 1 (HIV-1) (Wiley and Gummuluru, 2006), and porcine reproductive and respiratory syndrome virus (PRRSV) (Wang et al., 2017). Moreover, some viruses such as HIV-1 and human herpesvirus (HHV)-6 have been visualized by electron microscopy in MVBs and egress by the exosomal release pathway (Mori et al., 2008; Wiley and Gummuluru, 2006). On the other hand, hepatitis A virus (HAV) a nonenveloped virus of the *Picornaviridae* family, can egress from cells covered in host-derived membranes resembling exosomes (Feng et al., 2013).

In this sense, one possible explanation of the fact that the exosomes from DENV-infected C6/36 cells are larger than the ones secreted from uninfected cells is that the virus-like particles are found inside the exosomes. Certainly, the exosomes from DENV-infected mosquito cells isolated for us were able to infect naïve cells, supporting the idea that they are playing a pro-viral role. This result is consistent with the Vora et al. results (Vora et al., 2018), where the full-length genome of DENV 2, detected in the EVs from DENV-infected mosquito cells was infectious to naïve mosquito and mammalian cells. However, the presence of intact viral particles inside the EVs was not confirmed by Vora et al.

The observation of virus-like particles enclosed in exosomes derived from DENV-infected C6/36 cells could suggest that the virus egresses of the cells by an alternative mechanism. Moreover, the entry process of the viruses present in exosomes could be happening in a receptor-independent manner. In this sense, it has been suggested that the DENV particles entry into C6/36 cells could occur by a pathway different from the endosomal one (Farias et al., 2013). Additionally, the hijacking of mosquito cell membranes by DENV could facilitate the escape from neutralizing antibodies and host immune responses, promoting virus spread. However, these ideas require further investigation.

In summary, during DENV infection in the *A. albopictus* mosquito cells, a heterogeneous population of vesicles is produced. The specific population of exosomes released from DENV-infected mosquito cells, with a size range from 50 to 150 nm and positive to CD9, were larger than the ones from uninfected cells and they can infect naïve cells. All these results confirm that the exosomes are playing a role in DENV dissemination.

Acknowledgments

We want to thank Dr. Juan E. Ludert from CINVESTAV (Mexico) for their contributions to manuscript review. We thank Mariana Salas-Benito for the maintenance of cell lines and mice, and Anel Lagunes-

Guillén, Matilde García-Espitia, and Jaime Zarco for their technical assistance. This work was supported by the National Council of Science and Technology of Mexico (CONACYT) 220824 (RMA), Fundación Miguel Alemán (RMA), and Secretaría de Investigación y Posgrado (SIP 20151372) of Instituto Politécnico Nacional (JSB). Dr. Salas-Benito has a fellowship from Estímulo al Desempeño de los Investigadores (EDI) and Comisión de Operación y Fomento a las Actividades Académicas (COFAA) from Instituto Politécnico Nacional. José Manuel Reyes-Ruiz, Luis Adrian de Jesús, Noe Farfan-Morales, Arianna Hurtado-Monzón, and Juan Fidel Osuna-Ramos, received scholarships from Conacyt.

Appendix A. Supplementary data

Supplementary data associated with this article can be found, in the online version, at https://doi.org/10.1016/j.virusres.2019.03.015.

References

Ahmed, W., Philip, P.S., Tariq, S., Khan, G., 2014. Epstein-Barr virus-encoded small RNAs (EBERs) are present in fractions related to exosomes released by EBV-transformed cells. PLOS ONE 9, e99163. https://doi.org/10.1371/journal.pone.0099163.

An, Q., Ehlers, K., Kogel, K.-H., Bel, A.J.E.V., Hückelhoven, R., 2006a. Multivesicular compartments proliferate in susceptible and resistant MLA12-barley leaves in response to infection by the biotrophic powdery mildew fungus. New Phytol. 172, 563–576. https://doi.org/10.1111/j.1469-8137.2006.01844.x.

An, Q., Hückelhoven, R., Kogel, K.-H., van Bel, A.J.E., 2006b. Multivesicular bodies participate in a cell wall-associated defence response in barley leaves attacked by the pathogenic powdery mildew fungus. Cell Microbiol. 8, 1009–1019. https://doi.org/10.1111/j.1462-5822.2006.00683.x.

Andreu, Z., Yáñez-Mó, M., 2014. Tetraspanins in extracellular vesicle formation and function. Front. Immunol. 5. https://doi.org/10.3389/fimmu.2014.00442.

Ansari, M.A., Singh, V.V., Dutta, S., Veettil, M.V., Dutta, D., Chikoti, L., Lu, J., Everly, D., Chandran, B., 2013. Constitutive interferon-inducible protein 16-inflammasome activation during Epstein-Barr virus latency I, II, and III in B and epithelial cells. J. Virol. 87, 8606–8623. https://doi.org/10.1128/JVI.00805-13.

Azmi, A.S., Bao, B., Sarkar, F.H., 2013. Exosomes in cancer development, metastasis and drug resistance: a comprehensive review. Cancer Metastasis Rev. 32. https://doi.org/10.1007/s10555-013-9441-9.

Baixauli, F., López-Otín, C., Mittelbrunn, M., 2014. Exosomes and autophagy: coordinated mechanisms for the maintenance of cellular fitness. Front. Immunol. 5. https://doi.org/10.3389/fimmu.2014.00403.

Berditchevski, F., Odintsova, E., 2007. Tetraspanins as regulators of protein trafficking. Traffic Cph. Den. 8, 89–96. https://doi.org/10.1111/j.1600-0854.2006.00515.x.

Bissig, C., Gruenberg, J., 2014. ALIX and the multivesicular endosome: ALIX in Wonderland. Trends Cell Biol. 24, 19–25. https://doi.org/10.1016/j.tcb.2013.10.009.

Bobrie, A., Colombo, M., Krumeich, S., Raposo, G., Théry, C., 2012. Diverse subpopulations of vesicles secreted by different intracellular mechanisms are present in exosome preparations obtained by differential ultracentrifugation. J. Extracell. Vesicles 1. https://doi.org/10.3402/jev.v1i0.18397.

Bobrie, A., Colombo, M., Raposo, G., Théry, C., 2011. Exosome secretion: molecular mechanisms and roles in immune responses. Traffic 12, 1659–1668. https://doi.org/10.1111/j.1600-0854.2011.01225.x.

Braicu, C., Tomuleasa, C., Monroig, P., Cucuianu, A., Berindan-Neagoe, I., Calin, G.A., 2015. Exosomes as divine messengers: are they the Hermes of modern molecular oncology? Cell Death Differ. 22, 34–45. https://doi.org/10.1038/cdd.2014.130.

Bukong, T.N., Momen-Heravi, F., Kodys, K., Bala, S., Szabo, G., 2014. Exosomes from hepatitis C infected patients transmit HCV infection and contain replication competent viral RNA in complex with Ago2-miR122-HSP90. PLoS Pathog. 10, e1004424. https://doi.org/10.1371/journal.ppat.1004424.

Canitano, A., Venturi, G., Borghi, M., Ammendolia, M.G., Fais, S., 2013. Exosomes released in vitro from Epstein-Barr virus (EBV)-infected cells contain EBV-encoded latent phase mRNAs. Cancer Lett. 337, 193–199. https://doi.org/10.1016/j.canlet.2013.05.012.

Carayon, K., Chaoui, K., Ronzier, E., Lazar, I., Bertrand-Michel, J., Roques, V., Balor, S., Terce, F., Lopez, A., Salomé, L., Joly, E., 2011. Proteolipidic composition of exosomes changes during reticulocyte maturation. J. Biol. Chem. 286, 34426–34439. https://doi.org/10.1074/jbc.M111.257444.

Chang, Y., Finnemann, S.C., 2007. Tetraspanin CD81 is required for the αvβ5-integrin-dependent particle-binding step of RPE phagocytosis. J. Cell Sci. 120, 3053–3063. https://doi.org/10.1242/jcs.006361.

Chivet, M., Hemming, F., Pernet-Gallay, K., Fraboulet, S., Sadoul, R., 2012. Emerging role of neuronal exosomes in the central nervous system. Front. Physiol. 3, 145. https://doi.org/10.3389/fphys.2012.00145.

Cocucci, E., Racchetti, G., Meldolesi, J., 2009. Shedding microvesicles: artefacts no more. Trends Cell Biol. 19, 43–51. https://doi.org/10.1016/j.tcb.2008.11.003.

Colombo, M., Raposo, G., Théry, C., 2014. Biogenesis, secretion, and intercellular interactions of exosomes and other extracellular vesicles. Annu. Rev. Cell Dev. Biol. 30, 255–289. https://doi.org/10.1146/annurev-cellbio-101512-122326.

Cosset, F.-L., Dreux, M., 2014. HCV transmission by hepatic exosomes establishes a productive infection. J. Hepatol. 60, 674–675. https://doi.org/10.1016/j.jhep.2013.10.015.

Dargan, D.J., Subak-Sharpe, J.H., 1997. The effect of herpes simplex virus type 1 L-particles on virus entry, replication, and the infectivity of naked herpesvirus DNA. Virology 239, 378–388. https://doi.org/10.1006/viro.1997.8893.

Delabranche, X., Berger, A., Boisramé-Helms, J., Meziani, F., 2012. Microparticles and infectious diseases. Med. Mal. Infect. 42, 335–343. https://doi.org/10.1016/j.medmal.2012.05.011.

Edgar, J.R., 2016. Q&A: What are exosomes, exactly? BMC Biol. 14, 46. https://doi.org/10.1186/s12915-016-0268-z.

Escola, J.M., Kleijmeer, M.J., Stoorvogel, W., Griffith, J.M., Yoshie, O., Geuze, H.J., 1998. Selective enrichment of tetraspan proteins on the internal vesicles of multivesicular endosomes and on exosomes secreted by human B-lymphocytes. J. Biol. Chem. 273, 20121–20127.

Farias, K.J.S., Machado, P.R.L., da Fonseca, B.A.L., 2013. Chloroquine inhibits dengue virus type 2 replication in Vero cells but not in C6/36 cells. ScientificWorldJournal 2013, 282734. https://doi.org/10.1155/2013/282734.

Feng, Z., Hensley, L., McKnight, K.L., Hu, F., Madden, V., Ping, L., Jeong, S.-H., Walker, C., Lanford, R.E., Lemon, S.M., 2013. A pathogenic picornavirus acquires an envelope by hijacking cellular membranes. Nature 496, 367–371. https://doi.org/10.1038/nature12029.

Fevrier, B., Vilette, D., Archer, F., Loew, D., Faigle, W., Vidal, M., Laude, H., Raposo, G., 2004. Cells release prions in association with exosomes. Proc. Natl. Acad. Sci. U. S. A. 101, 9683–9688. https://doi.org/10.1073/pnas.0308413101.

Gheinani, A.H., Vögeli, M., Baumgartner, U., Vassella, E., Draeger, A., Burkhard, F.C., Monastyrskaya, K., 2018. Improved isolation strategies to increase the yield and purity of human urinary exosomes for biomarker discovery. Sci. Rep. 8, 3945. https://doi.org/10.1038/s41598-018-22142-x.

Gould, E., Clegg, J., 1991. Growth, titration and purification of alphaviruses and flaviviruses. In: Mahy, B.W.J. (Ed.), Virol. Pract. Approach. IRL Press, Oxford, pp. 43–78.

Greenhill, C., 2013. Hepatitis: new route of HCV transmission. Nat. Rev. Gastroenterol. Hepatol. 10, 504. https://doi.org/10.1038/nrgastro.2013.148.

Guzman, M.G., Harris, E., 2015. Dengue. Lancet 385, 453–465. https://doi.org/10.1016/S0140-6736(14)60572-9.

Hemler, M.E., 2005. Tetraspanin functions and associated microdomains. Nat. Rev. Mol. Cell Biol. 6, 801–811. https://doi.org/10.1038/nrm1736.

Hemler, M.E., 2001. Specific tetraspanin functions. J. Cell Biol. 155, 1103–1108. https://doi.org/10.1083/jcb.200108061.

Hyenne, V., Apaydin, A., Rodriguez, D., Spiegelhalter, C., Hoff-Yoessle, S., Diem, M., Tak, S., Lefebvre, O., Schwab, Y., Goetz, J.G., Labouesse, M., 2015. RAL-1 controls multivesicular body biogenesis and exosome secretion. J. Cell Biol. 211, 27–37. https://doi.org/10.1083/jcb.201504136.

Igarashi, A., 1978. Isolation of a Singh's *Aedes albopictus* cell clone sensitive to Dengue and Chikungunya viruses. J. Gen. Virol. 40, 531–544. https://doi.org/10.1099/0022-1317-40-3-531.

Ikeda, M., Longnecker, R., 2007. Cholesterol is critical for Epstein-Barr virus latent membrane protein 2A trafficking and protein stability. Virology 360, 461–468. https://doi.org/10.1016/j.virol.2006.10.046.

Imhof, I., Gasper, W.J., Derynck, R., 2008. Association of tetraspanin CD9 with transmembrane TGFα confers alterations in cell-surface presentation of TGFα and cytoskeletal organization. J. Cell Sci. 121, 2265–2274. https://doi.org/10.1242/jcs.021717.

Jankovičová, J., Simon, M., Antalíková, J., Cupperová, P., Michalková, K., 2015. Role of tetraspanin CD9 molecule in fertilization of mammals. Physiol. Res. 64, 279–293.

Jella, K.K., Yu, L., Yue, Q., Friedman, D., Duke, B.J., Alli, A.A., 2016. Exosomal GAPDH from proximal tubule cells regulate ENaC activity. PLOS ONE 11. https://doi.org/10.1371/journal.pone.0165763.

Juárez-Martínez, A.B., Vega-Almeida, T.O., Salas-Benito, M., García-Espitia, M., Nova-Ocampo, M.D., Ángel, R.M. del, Salas-Benito, J.S., 2012. Detection and sequencing of defective viral genomes in C6/36 cells persistently infected with dengue virus 2. Arch. Virol. 158, 583–599. https://doi.org/10.1007/s00705-012-1525-2.

Junjhon, J., Pennington, J.G., Edwards, T.J., Perera, R., Lanman, J., Kuhn, R.J., 2014. Ultrastructural characterization and three-dimensional architecture of replication sites in dengue virus-infected mosquito cells. J. Virol. 88, 4687–4697. https://doi.org/10.1128/JVI.00118-14.

Kaji, K., Takeshita, S., Miyake, K., Takai, T., Kudo, A., 2001. Functional association of CD9 with the Fcγ receptors in Macrophages. J. Immunol. 166, 3256–3265. https://doi.org/10.4049/jimmunol.166.5.3256.

Kalluri, R., 2016. The biology and function of exosomes in cancer. J. Clin. Invest. 126, 1208–1215. https://doi.org/10.1172/JCI81135.

Kalra, H., Simpson, R.J., Ji, H., Aikawa, E., Altevogt, P., Askenase, P., Bond, V.C., Borràs, F.E., Breakefield, X., Budnik, V., Buzas, E., Camussi, G., Clayton, A., Cocucci, E., Falcon-Perez, J.M., Gabrielsson, S., Gho, Y.S., Gupta, D., Harsha, H.C., Hendrix, A., Hill, A.F., Inal, J.M., Jenster, G., Krämer-Albers, E.-M., Lim, S.K., Llorente, A., Lötvall, J., Marcilla, A., Mincheva-Nilsson, L., Nazarenko, I., Nieuwland, R., Nolte-'t Hoen, E.N.M., Pandey, A., Patel, T., Piper, M.G., Pluchino, S., Prasad, T.S.K., Rajendran, L., Raposo, G., Record, M., Reid, G.E., Sánchez-Madrid, F., Schiffelers, R.M., Siljander, P., Stensballe, A., Stoorvogel, W., Taylor, D., Thery, C., Valadi, H., van Balkom, B.W.M., Vázquez, J., Vidal, M., Wauben, M.H.M., Yáñez-Mó, M., Zoeller, M., Mathivanan, S., 2012. Vesiclepedia: a compendium for extracellular vesicles with continuous community annotation. PLoS Biol. 10. https://doi.org/10.1371/journal.pbio.1001450.

Keerthikumar, S., Chisanga, D., Ariyaratne, D., Saffar, H.A., Anand, S., Zhao, K., Samuel, M., Pathan, M., Jois, M., Chilamkurti, N., Gangoda, L., Mathivanan, S., 2016. ExoCarta: a web-based compendium of exosomal cargo. J. Mol. Biol. 428, 688–692. https://doi.org/10.1016/j.jmb.2015.09.019.

Kitadokoro, K., Bordo, D., Galli, G., Petracca, R., Falugi, F., Abrignani, S., Grandi, G., Bolognesi, M., 2001. CD81 extracellular domain 3D structure: insight into the tetraspanin superfamily structural motifs. EMBO J. 20, 12–18. https://doi.org/10.1093/emboj/20.1.12.

Klibi, J., Niki, T., Riedel, A., Pioche-Durieu, C., Souquere, S., Rubinstein, E., Moulec, S.L., Guigay, J., Hirashima, M., Guemira, F., Adhikary, D., Mautner, J., Busson, P., 2009. Blood diffusion and Th1-suppressive effects of galectin-9-containing exosomes released by Epstein-Barr virus-infected nasopharyngeal carcinoma cells. Blood 113, 1957–1966. https://doi.org/10.1182/blood-2008-02-142596.

Kraemer, M.U.G., Sinka, M.E., Duda, K.A., Mylne, A.Q.N., Shearer, F.M., Barker, C.M., Moore, C.G., Carvalho, R.G., Coelho, G.E., Van Bortel, W., Hendrickx, G., Schaffner, F., Elyazar, I.R.F., Teng, H.-J., Brady, O.J., Messina, J.P., Pigott, D.M., Scott, T.W., Smith, D.L., Wint, G.R.W., Golding, N., Hay, S.I., 2015. The global distribution of the arbovirus vectors *Aedes aegypti* and *Ae. albopictus*. eLife 4, e08347. https://doi.org/10.7554/eLife.08347.

Kuhn, R.J., Zhang, W., Rossmann, M.G., Pletnev, S.V., Corver, J., Lenches, E., Jones, C.T., Mukhopadhyay, S., Chipman, P.R., Strauss, E.G., Baker, T.S., Strauss, J.H., 2002. Structure of dengue virus: implications for flavivirus organization, maturation, and fusion. Cell 108, 717–725.

Kuno, G., Oliver, A., 1989. Maintaining mosquito cell lines at high temperatures: effects on the replication of flaviviruses. IIn Vitro Cell. Dev. Biol. 25, 193–196.

Levy, S., 2014. Function of the tetraspanin molecule CD81 in B and T cells. Immunol. Res. 58, 179–185. https://doi.org/10.1007/s12026-014-8490-7.

Li, M., Zeringer, E., Barta, T., Schageman, J., Cheng, A., Vlassov, A.V., 2014. Analysis of the RNA content of the exosomes derived from blood serum and urine and its potential as biomarkers. Philos. Trans. R. Soc. B: Biol. Sci. 369. https://doi.org/10.1098/rstb.2013.0502.

Li, P., Kaslan, M., Lee, S.H., Yao, J., Gao, Z., 2017. Progress in exosome isolation techniques. Theranostics 7, 789–804. https://doi.org/10.7150/thno.18133.

Longatti, A., Boyd, B., Chisari, F.V., 2015. Virion-independent transfer of replication-competent hepatitis C virus RNA between permissive cells. J. Virol. 89, 2956–2961. https://doi.org/10.1128/JVI.02721-14.

Martins, S.T., Kuczera, D., Lötvall, J., Bordignon, J., Alves, L.R., 2018. Characterization of dendritic cell-derived extracellular vesicles during dengue virus infection. Front. Microbiol. 9. https://doi.org/10.3389/fmicb.2018.01792.

Mathivanan, S., Lim, J.W.E., Tauro, B.J., Ji, H., Moritz, R.L., Simpson, R.J., 2010. Proteomics analysis of A33 immunoaffinity-purified exosomes released from the human colon tumor cell line LIM1215 reveals a tissue-specific protein signature. Mol. Cell. Proteomics 9, 197–208. https://doi.org/10.1074/mcp.M900152-MCP200.

Matsuo, H., Chevallier, J., Mayran, N., Blanc, I.L., Ferguson, C., Fauré, J., Blanc, N.S., Matile, S., Dubochet, J., Sadoul, R., Parton, R.G., Vilbois, F., Gruenberg, J., 2004. Role of LBPA and alix in multivesicular liposome formation and endosome organization. Science 303, 531–534. https://doi.org/10.1126/science.1092425.

Mears, R., Craven, R.A., Hanrahan, S., Totty, N., Upton, C., Young, S.L., Patel, P., Selby, P.J., Banks, R.E., 2004. Proteomic analysis of melanoma-derived exosomes by two-dimensional polyacrylamide gel electrophoresis and mass spectrometry. Proteomics 4, 4019–4031. https://doi.org/10.1002/pmic.200400876.

Meckes, D.G., 2015. Exosomal communication goes viral. J. Virol. 89, 5200–5203. https://doi.org/10.1128/JVI.02470-14.

Meckes, D.G., Gunawardena, H.P., Dekroon, R.M., Heaton, P.R., Edwards, R.H., Ozgur, S., Griffith, J.D., Damania, B., Raab-Traub, N., 2013. Modulation of B-cell exosome proteins by gamma herpesvirus infection. Proc. Natl. Acad. Sci. U. S. A. 110, E2925–E2933. https://doi.org/10.1073/pnas.1303906110.

Meckes, D.G., Shair, K.H.Y., Marquitz, A.R., Kung, C.-P., Edwards, R.H., Raab-Traub, N., 2010. Human tumor virus utilizes exosomes for intercellular communication. Proc. Natl. Acad. Sci. U. S. A. 107, 20370–20375. https://doi.org/10.1073/pnas.1014194107.

Meyer, K., Kwon, Y.-C., Liu, S., Hagedorn, C.H., Ray, R.B., Ray, R., 2015. Interferon-α inducible protein 6 impairs EGFR activation by CD81 and inhibits hepatitis C virus infection. Sci. Rep. 5, 9012. https://doi.org/10.1038/srep09012.

Möbius, W., Ohno-Iwashita, Y., van Donselaar, E.G., Oorschot, V.M.J., Shimada, Y., Fujimoto, T., Heijnen, H.F.G., Geuze, H.J., Slot, J.W., 2002. Immunoelectron microscopic localization of cholesterol using biotinylated and non-cytolytic perfringolysin O. J. Histochem. Cytochem. Off. J. Histochem. Soc. 50, 43–55. https://doi.org/10.1177/002215540205000105.

Mori, Y., Koike, M., Moriishi, E., Kawabata, A., Tang, H., Oyaizu, H., Uchiyama, Y., Yamanishi, K., 2008. Human herpesvirus-6 induces MVB formation, and virus egress occurs by an exosomal release pathway. Traffic Cph. Den. 9, 1728–1742. https://doi.org/10.1111/j.1600-0854.2008.00796.x.

Muller, L., Hong, C.-S., Stolz, D.B., Watkins, S.C., Whiteside, T.L., 2014. Isolation of biologically-active exosomes from human plasma. J. Immunol. Methods 411, 55–65. https://doi.org/10.1016/j.jim.2014.06.007.

Osuna-Ramos, J.F., Reyes-Ruiz, J.M., del Ángel, R.M., 2018. The role of host cholesterol during flavivirus infection. Front. Cell. Infect. Microbiol. 8. https://doi.org/10.3389/fcimb.2018.00388.

Palanisamy, V., Sharma, S., Deshpande, A., Zhou, H., Gimzewski, J., Wong, D.T., 2010. Nanostructural and transcriptomic analyses of human saliva derived exosomes. PLOS ONE 5, e8577. https://doi.org/10.1371/journal.pone.0008577.

Pan, B.T., Johnstone, R.M., 1983. Fate of the transferrin receptor during maturation of sheep reticulocytes in vitro: selective externalization of the receptor. Cell 33, 967–978.

Pandey, U.B., Nie, Z., Batlevi, Y., McCray, B.A., Ritson, G.P., Nedelsky, N.B., Schwartz, S.L., DiProspero, N.A., Knight, M.A., Schuldiner, O., Padmanabhan, R., Hild, M., Berry, D.L., Garza, D., Hubbert, C.C., Yao, T.-P., Baehrecke, E.H., Taylor, J.P., 2007. HDAC6 rescues neurodegeneration and provides an essential link between autophagy and the UPS. Nature 447, 859–863. https://doi.org/10.1038/nature05853.

Pegtel, D.M., van de Garde, M.D.B., Middeldorp, J.M., 2011. Viral miRNAs exploiting the endosomal–exosomal pathway for intercellular cross-talk and immune evasion. Biochim. Biophys. Acta 1809, 715–721. https://doi.org/10.1016/j.bbagrm.2011.08.002.

Pisitkun, T., Shen, R.-F., Knepper, M.A., 2004. Identification and proteomic profiling of exosomes in human urine. Proc. Natl. Acad. Sci. U. S. A. 101, 13368–13373. https://doi.org/10.1073/pnas.0403453101.

Raab-Traub, N., Dittmer, D.P., 2017. Viral effects on the content and function of extracellular vesicles. Nat. Rev. Microbiol. 15, 559–572. https://doi.org/10.1038/nrmicro.2017.60.

Raghow, R.S., Grace, T.D., Filshie, B.K., Bartley, W., Dalgarno, L., 1973. Ross River virus replication in cultured mosquito and mammalian cells: virus growth and correlated ultrastructural changes. J. Gen. Virol. 21, 109–122. https://doi.org/10.1099/0022-1317-21-1-109.

Ramakrishnaiah, V., Thumann, C., Fofana, I., Habersetzer, F., Pan, Q., de Ruiter, P.E., Willemsen, R., Demmers, J.A.A., Stalin Raj, V., Jenster, G., Kwekkeboom, J., Tilanus, H.W., Haagmans, B.L., Baumert, T.F., van der Laan, L.J.W., 2013. Exosome-mediated transmission of hepatitis C virus between human hepatoma Huh7.5 cells. Proc. Natl. Acad. Sci. U. S. A. 110, 13109–13113. https://doi.org/10.1073/pnas.1221899110.

Regev-Rudzki, N., Wilson, D.W., Carvalho, T.G., Sisquella, X., Coleman, B.M., Rug, M., Bursac, D., Angrisano, F., Gee, M., Hill, A.F., Baum, J., Cowman, A.F., 2013. Cell–cell communication between malaria-infected red blood cells via exosome-like vesicles. Cell 153, 1120–1133. https://doi.org/10.1016/j.cell.2013.04.029.

Reyes-Ruiz, J.M., Osuna-Ramos, J.F., Bautista-Carbajal, P., Jaworski, E., Soto-Acosta, R., Cervantes-Salazar, M., Angel-Ambrocio, A.H., Castillo-Munguía, J.P., Chávez-Munguía, B., De Nova-Ocampo, M., Routh, A., del Ángel, R.M., Salas-Benito, J.S., 2019. Mosquito cells persistently infected with dengue virus produce viral particles with host-dependent replication. Virology 531, 1–18. https://doi.org/10.1016/j.virol.2019.02.018.

Reyes-Ruiz, J.M., Osuna-Ramos, J.F., Cervantes-Salazar, M., Lagunes Guillen, A.E., Chávez-Munguía, B., Salas-Benito, J.S., Del Ángel, R.M., 2018. Strand-like structures and the nonstructural proteins 5, 3 and 1 are present in the nucleus of mosquito cells infected with dengue virus. Virology 515, 74–80. https://doi.org/10.1016/j.virol.2017.12.014.

Scotti, E., Calamai, M., Goulbourne, C.N., Zhang, L., Hong, C., Lin, R.R., Choi, J., Pilch, P.F., Fong, L.G., Zou, P., Ting, A.Y., Pavone, F.S., Young, S.G., Tontonoz, P., 2013. IDOL stimulates clathrin-independent endocytosis and multivesicular body-mediated lysosomal degradation of the low-density lipoprotein receptor. Mol. Cell. Biol. 33, 1503–1514. https://doi.org/10.1128/MCB.01716-12.

Sharma, S., Rasool, H.I., Palanisamy, V., Mathisen, C., Schmidt, M., Wong, D.T., Gimzewski, J.K., 2010. Structural–mechanical characterization of nanoparticles – exosomes in human saliva, using correlative AFM, FESEM and force spectroscopy. ACS Nano 4, 1921–1926. https://doi.org/10.1021/nn901824n.

Simmons, C.P., Farrar, J.J., Nguyen, van, V.C., Wills, B., 2012. Dengue. N. Engl. J. Med. 366, 1423–1432. https://doi.org/10.1056/NEJMra1110265.

Simons, M., Raposo, G., 2009. Exosomes – vesicular carriers for intercellular communication. Curr. Opin. Cell Biol. 21, 575–581. https://doi.org/10.1016/j.ceb.2009.03.007.

Steinbichler, T.B., Dudás, J., Riechelmann, H., Skvortsova, I.-I., 2017. The role of exosomes in cancer metastasis. Semin. Cancer Biol. Progr. Biol. Understand. Cancer Metastasis 44, 170–181. https://doi.org/10.1016/j.semcancer.2017.02.006.

Stipp, C.S., Kolesnikova, T.V., Hemler, M.E., 2003. Functional domains in tetraspanin proteins. Trends Biochem. Sci. 28, 106–112. https://doi.org/10.1016/S0968-0004(02)00014-2.

Tamboli, I.Y., Barth, E., Christian, L., Siepmann, M., Kumar, S., Singh, S., Tolksdorf, K., Heneka, M.T., Lütjohann, D., Wunderlich, P., Walter, J., 2010. Statins promote the degradation of extracellular amyloid β-peptide by microglia via stimulation of exosome-associated insulin-degrading enzyme (IDE) secretion. J. Biol. Chem. 285, 37405–37414. https://doi.org/10.1074/jbc.M110.149468.

Tamura, K., Peterson, D., Peterson, N., Stecher, G., Nei, M., Kumar, S., 2011. MEGA5: molecular evolutionary genetics analysis using maximum likelihood, evolutionary distance, and maximum parsimony methods. Mol. Biol. Evol. 28, 2731–2739. https://doi.org/10.1093/molbev/msr121.

Théry, C., 2011. Exosomes: secreted vesicles and intercellular communications. F1000 Biol. Rep. 3. https://doi.org/10.3410/B3-15.

Théry, C., Amigorena, S., Raposo, G., Clayton, A., 2006. Isolation and characterization of exosomes from cell culture supernatants and biological fluids. Curr. Protoc. Cell Biol. https://doi.org/10.1002/0471143030.cb0322s30. (Chapter 3, Unit 3.22).

Théry, C., Regnault, A., Garin, J., Wolfers, J., Zitvogel, L., Ricciardi-Castagnoli, P., Raposo, G., Amigorena, S., 1999. Molecular characterization of dendritic cell-derived exosomes. J. Cell Biol. 147, 599–610.

Todres, E., Nardi, J.B., Robertson, H.M., 2000. The tetraspanin superfamily in insects. Insect Mol. Biol. 9, 581–590.

Urbanelli, L., Magini, A., Buratta, S., Brozzi, A., Sagini, K., Polchi, A., Tancini, B., Emiliani, C., 2013. Signaling Pathways in exosomes biogenesis, secretion and fate. Genes 4, 152–170. https://doi.org/10.3390/genes4020152.

van Niel, G., Raposo, G., Candalh, C., Boussac, M., Hershberg, R., Cerf-Bensussan, N., Heyman, M., 2001. Intestinal epithelial cells secrete exosome-like vesicles. Gastroenterology 121, 337–349.

van Spriel, A.B., 2011. Tetraspanins in the humoral immune response. Biochem. Soc. Trans. 39, 512–517. https://doi.org/10.1042/BST0390512.

Von Bartheld, C.S., Altick, A.L., 2011. Multivesicular bodies in neurons: distribution, protein content, and trafficking functions. Prog. Neurobiol. 93, 313–340. https://doi.org/10.1016/j.pneurobio.2011.01.003.

Vora, A., Zhou, W., Londono-Renteria, B., Woodson, M., Sherman, M.B., Colpitts, T.M., Neelakanta, G., Sultana, H., 2018. Arthropod EVs mediate dengue virus transmission

through interaction with a tetraspanin domain containing glycoprotein Tsp29Fb. Proc. Natl. Acad. Sci. U. S. A. https://doi.org/10.1073/pnas.1720125115. 201720125.

Wang, T., Fang, L., Zhao, F., Wang, D., Xiao, S., 2017. Exosomes mediate intercellular transmission of porcine reproductive and respiratory syndrome virus (PRRSV). J. Virol. https://doi.org/10.1128/JVI.01734-17.

Welsch, S., Miller, S., Romero-Brey, I., Merz, A., Bleck, C.K.E., Walther, P., Fuller, S.D., Antony, C., Krijnse-Locker, J., Bartenschlager, R., 2009. Composition and three-dimensional architecture of the dengue virus replication and assembly sites. Cell Host Microbe 5, 365–375. https://doi.org/10.1016/j.chom.2009.03.007.

White, I.J., Bailey, L.M., Aghakhani, M.R., Moss, S.E., Futter, C.E., 2006. EGF stimulates annexin 1-dependent inward vesiculation in a multivesicular endosome subpopulation. EMBO J. 25, 1–12. https://doi.org/10.1038/sj.emboj.7600759.

Wiley, R.D., Gummuluru, S., 2006. Immature dendritic cell-derived exosomes can mediate HIV-1 trans infection. Proc. Natl. Acad. Sci. U. S. A. 103, 738–743. https://doi.org/10.1073/pnas.0507995103.

Willms, E., Johansson, H.J., Mäger, I., Lee, Y., Blomberg, K.E.M., Sadik, M., Alaarg, A., Smith, C.I.E., Lehtiö, J., Andaloussi, S.E., Wood, M.J.A., Vader, P., 2016. Cells release subpopulations of exosomes with distinct molecular and biological properties. Sci. Rep. 6, 22519. https://doi.org/10.1038/srep22519.

Yang, C., Guo, W.-B., Zhang, W.-S., Bian, J., Yang, J.-K., Zhou, Q.-Z., Chen, M.-K., Peng, W., Qi, T., Wang, C.-Y., Liu, C.-D., 2017. Comprehensive proteomics analysis of exosomes derived from human seminal plasma. Andrology 5, 1007–1015. https://doi.org/10.1111/andr.12412.

Zhou, W., Woodson, M., Neupane, B., Bai, F., Sherman, M.B., Choi, K.H., Neelakanta, G., Sultana, H., 2018. Exosomes serve as novel modes of tick-borne flavivirus transmission from arthropod to human cells and facilitates dissemination of viral RNA and proteins to the vertebrate neuronal cells. PLoS Pathog. 14, e1006764. https://doi.org/10.1371/journal.ppat.1006764.

Zhu, X., He, Z., Yuan, J., Wen, W., Huang, X., Hu, Y., Lin, C., Pan, J., Li, R., Deng, H., Liao, S., Zhou, R., Wu, J., Li, J., Li, M., 2015. IFITM3-containing exosome as a novel mediator for anti-viral response in dengue virus infection. Cell. Microbiol. 17, 105–118. https://doi.org/10.1111/cmi.12339.

Zimmerman, B., Kelly, B., McMillan, B.J., Seegar, T.C.M., Dror, R.O., Kruse, A.C., Blacklow, S.C., 2016. Crystal structure of a full-length human tetraspanin reveals a cholesterol-binding pocket. Cell 167https://doi.org/10.1016/j.cell.2016.09.056. 1041–1051.e11.

Zitvogel, L., Regnault, A., Lozier, A., Wolfers, J., Flament, C., Tenza, D., Ricciardi-Castagnoli, P., Raposo, G., Amigorena, S., 1998. Eradication of established murine tumors using a novel cell-free vaccine: dendritic cell derived exosomes. Nat. Med. 4, 594–600. https://doi.org/10.1038/nm0598-594.